AD-A171 328 QUALITY CONTROL OF TRUE HEIGHT PROFILES OBTAINED AUTOMATICALLY FROM DIGIT..(U) LOWELL UNIV MA CENTER FOR ATMOSPHERIC RESEARCH L F MCNAMARA MAY 82 ULRF-432/CAR 1/1

UNCLASSIFIED AFGL-TR-86-0098 F19628-83-C-0092 F/G 4/1 NL

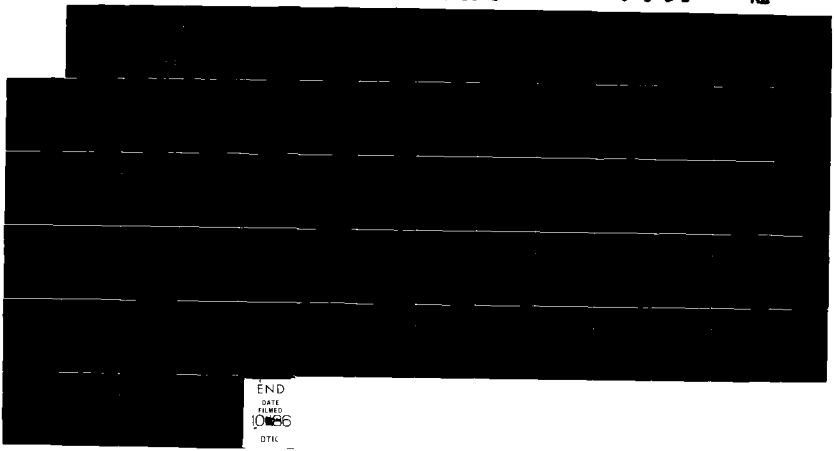

END
DATE FILMED
10-86
DTIC

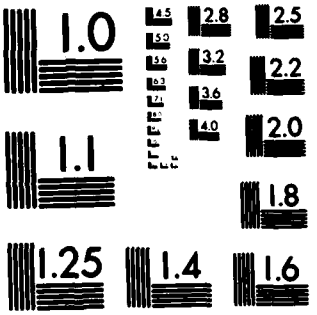

CROCOPY RESOLUTION TEST CHART
NATIONAL BUREAU OF STANDARDS-1963-A

(12)

AFGL-TR-86-0098

QUALITY CONTROL OF TRUE HEIGHT PROFILES OBTAINED AUTOMATICALLY FROM DIGITAL IONOGRAMS

Leo F. McNamara

University of Lowell
Center for Atmospheric Research
450 Aiken Street
Lowell, Massachusetts 01854

May 1986

Scientific Report No. 3

AIR FORCE GEOPHYSICS LABORATORY
AIR FORCE SYSTEMS COMMAND
UNITED STATES AIR FORCE
HANSCOM AFB, MASSACHUSETTS 01731

"This technical report has been reviewed and is approved for publication"

JURGEN BUCHAU
Alternate Contract Manager
Ionospheric Effects Branch

HERBERT C. CARLSON, Chief
Ionospheric Effects Branch
Ionospheric Physics Division

FOR THE COMMANDER

ROBERT A. SKRIVANEK
Director
Ionospheric Physics Division

This report has been reviewed by the ESD Public Affairs Office (PA) and is releasable to the National Technical Information Service (NTIS).

Qualified requestors may obtain additional copies from the Defense Technical Information Center. All others should apply to the National Techncial Information Service.

If your address has changed, or if you wish to be removed from the mailing list, or if the addressee is no longer employed by your organization, please notify AFGL/DAA, Hanscom AFB, MA 01731. This will assist us in maintaining a current mailing list.

UNCLASSIFIED

SECURITY CLASSIFICATION OF THIS PAGE (When Data Entered)

REPORT DOCUMENTATION PAGE		READ INSTRUCTIONS BEFORE COMPLETING FORM
1. REPORT NUMBER AFGL-TR-86-0098	2. GOVT ACCESSION NO. ADA 171 328	3. RECIPIENT'S CATALOG NUMBER
4. TITLE (and Subtitle) QUALITY CONTROL OF TRUE HEIGHT PROFILES OBTAINED AUTOMATICALLY FROM DIGITAL IONOGRAMS		5. TYPE OF REPORT & PERIOD COVERED Scientific No. 3
		6. PERFORMING ORG. REPORT NUMBER ULRF-432/CAR
7. AUTHOR(s) Leo F. McNamara		8. CONTRACT OR GRANT NUMBER(s) F19628-83-C-0092
9. PERFORMING ORGANIZATION NAME AND ADDRESS University of Lowell, Center for Atmospheric Research, 450 Aiken Street, Lowell, Massachusetts 01854		10. PROGRAM ELEMENT, PROJECT, TASK AREA & WORK UNIT NUMBERS 62101F 464308AD
11. CONTROLLING OFFICE NAME AND ADDRESS Air Force Geophysics Laboratory Hanscom AFB, MA 01731 Contract Monitor: J. B. Waaramaa (LIS)		12. REPORT DATE May 1986
		13. NUMBER OF PAGES 72
14. MONITORING AGENCY NAME & ADDRESS(if different from Controlling Office)		15. SECURITY CLASS. (of this report) UNCLASSIFIED
		15a. DECLASSIFICATION DOWNGRADING SCHEDULE

16. DISTRIBUTION STATEMENT (of this Report)

Approved for public release; distribution unlimited.

17. DISTRIBUTION STATEMENT (of the abstract entered in Block 20, if different from Report)

18. SUPPLEMENTARY NOTES

19. KEY WORDS (Continue on reverse side if necessary and identify by block number)

Ionosphere
Electron Density Profile
Ionogram
Autoscaling
ARTIST
Digisonde

20. ABSTRACT (Continue on reverse side if necessary and identify by block number)

The automatic scaling and determination of true height profiles from digital vertical ionograms are key elements in the ever increasing use of digital ionosondes for real-time HF propagation prediction purposes and for the accumulation of valuable computer-accessible scientific data. The N(h) profiles passed on to the propagation prediction programs or to scientific archives must be reliable, and if not, an indication to this effect must be

DD FORM 1 JAN 73 1473 EDITION OF 1 NOV 65 IS OBSOLETE

UNCLASSIFIED

SECURITY CLASSIFICATION OF THIS PAGE (When Data Entered)

20. ABSTRACT

passed on instead. This procedure must be made automatic, in view of the large amounts of data and short time scales involved.

In general, it is extremely difficult to tell that a profile is incorrect simply by looking at it in conjunction with the ionogram, since the relationship between the two is very complex. This report describes five simple techniques which can be used automatically to indicate the reliability of the deduced N(h) profile. A study of about 1000 auto-scaled Digisonde ionograms from five North American stations has shown that a profile may safely be rejected as unreliable if several of the techniques separately indicate that it is unreliable.

In all the cases considered, the errors arose from incorrect scaling of the ionograms by the auto-scaling software, for various ionospheric and non-ionospheric reasons, or from minor technical mistakes.

TABLE OF CONTENTS

LIST OF FIGURES

LIST OF TABLES

LIST OF TABLES (Continued)

LIST OF TABLES (Continued)

LIST OF TABLES (Continued)

1.0 INTRODUCTION

The results presented here arose out of a more general study which had four main aims:

1. To compare the relative merits of the N(h) analysis technique currently used with the ionogram traces scaled automatically by the ARTIST software [Reinisch and Huang, 1983; Reinisch et al, 1984], and the generalized polynomial analysis technique POLAN [Titheridge, 1985], using the same ARTIST-identified ionogram traces.

2. To determine how robust POLAN is in handling auto-scaled data.

3. To investigate techniques for indicating the quality of the deduced N(h) profile.

4. To investigate the accuracy of simple techniques for deriving the height of the peak of the F2 layer using routinely scaled ionospheric parameters.

The program POLAN was found to be one of the best two methods studied by an URSI Working Group set up to compare all methods then available [McNamara, 1978]. Since then the program has been extensively documented and improved [Titheridge, 1985]. The Reinisch and Huang technique has been found to be reliable under most conditions, but some difficulties have been encountered in the treatment of valleys. Recent tests at the University of Lowell Center for Atmospheric Research (ULCAR) on analytic and actual ionograms have shown that POLAN makes better use of physical models and constraints to prevent unreasonable solutions, as well as offering the possibility of using extraordinary ray data where it is appropriate to do so. ULCAR has therefore decided to adopt POLAN for future requirements.

It is essential for automatic operation that the N(h) analysis technique does not cause a "system crash" when it encounters bad data. Instead, the technique should try firstly to make some reasonable modifications to the data determined to be bad. If the data are found to be too physically unreal, the analysis should be terminated deliberately and control returned to the main program. POLAN had no difficulties satisfying these requirements, and did not once cause a system crash in the analysis of over 1000 auto-scaled ionograms, using Professional Fortran on an IBM PC/AT. [This is the micro-computer which the Digisonde uses for the ARTIST scaling.] Thus the robustness of POLAN for use with ARTIST-scaled data has been established.

The third aim of the present study was to develop techniques for checking the quality of the deduced N(h) profile. Such a quality check is essential for applications in which the profiles are passed, without human intervention, on to a later software package or archived in a data base for scientific purposes. The investigation of the accuracy of simple techniques for determining the altitude of the F2 layer peak was prompted by a recommendation from a meeting in Louvain, Belgium, in late 1985, of the URSI-COSPAR working group on the International Reference Ionosphere. The third and fourth aims of this study are in fact very closely interconnected, and it is these which we shall be concentrating on.

We have analyzed about 1000 Digisonde ionograms from the five North American stations listed in Table 1 - Lowell, Massachusetts; Argentia, Newfoundland; Goose Bay, Labrador; Richfield, Utah; and Erie, Colorado. The ionograms were chosen on the basis of their ready availability, and do not necessarily represent a statistically perfect sample. As well as obtaining the N(h) profile for each ionogram using

STATION	LAT.	LON. (E)	DIP	FB (O)	EPOCH
Lowell	42.6	288.7	70.4	1.56	Mar. 86
Argentia	47.3	306.0	69.6	1.49	Feb. 86
Goose Bay	53.3	299.7	75.1	1.58	Jan. 85
Richfield	39.0	248.0	65.0	1.50	Sep. 84
Erie	40.0	254.7	67.3	1.55	Mar. 85 Apr. 85

Table 1. The five stations for which ionograms were analyzed. The magnetic dip angles (DIP) and electron gyrofrequency at the ground (FB) were obtained using the International Geomagnetic Reference Field.

POLAN, we have also recalculated the value of M(3000)F2, and calculated the values of the peak height hmF2 given by the simple Dudeney [1983] model of the ionosphere, and the value of the semi-thickness ymF2 given by the similar CCIR [1980] model.

The present analysis, together with the normal output from POLAN, suggests that the following five features may be used to indicate the reliability of the N(h) profile given by POLAN using ARTIST auto-scaled data:

1. The frequency which determines the value of M(3000)F2.
2. The difference between the POLAN and Dudeney values of hmF2.
3. The difference between the POLAN and CCIR values of ymF2.
4. The standard error in the calculated value of hmF2.
5. The use by POLAN of a model value for the F2-layer scale height.

The standard error and the model scale height are discussed in paragraphs 4.4 and 4.5.

It would also be possible to keep track of the adjustments which POLAN automatically makes to any physically inconsistent input data in order to derive an acceptable N(h) profile. Such adjustments occur quite often with the auto-scaled data with 5 km range bins provided by the Digisonde 256, especially when the trace is horizontal or nearly so. Most of these adjustments are found to be perfectly acceptable in retrospect, but some have been found to obscure the fact that the ionogram was badly scaled by ARTIST. This option will be considered at a later date.

The results of the N(h) analyses which are relevant to the present study are listed in Tables 2 to 7. The

parameters listed in the tables are explained in later sections, and only a preliminary scan of the DIFF, STER and M columns is necessary at this point. The reader should look for the occurrence of large values of DIFF and STERR, and for M values set negative.

Experience will show what weights to give to each of the five indicators. Care must be taken at all times to ensure that an unusual ionogram does not get rejected simply because the ionogram itself was unusual - it must be the scaling which leads to unacceptable values of the quality indicators.

All ionogram analyses were performed using the MODE=5 option recommended by Titheridge for general use. Ionograms for which ARTIST provided fewer than five points per layer (covering 0.5 MHz) were ignored. Nighttime ionograms covering such a short frequency range could be expected a priori to yield uncertain N(h) profiles. Ionograms with fewer than five points in the E layer were also ignored, since POLAN requires this many points for a MODE=5 analysis. In any future study, extra points should be interpolated using the E-layer parabola fitted to the data by ARTIST.

LOWELL March 1986 Universal Time

TIME	X	dM	POL	DUD	DIFF	STER	M
2229	3.17	0.12	241.8	237.6	4.3	11.4	3.53
2239	3.24	0.11	239.6	243.0	-3.5	9.7	3.48
23 8	3.27	0.11	243.7	253.8	-10.1	1.1	3.38
2319	3.00	0.13	242.0	251.0	-9.0	7.6	3.38
2329	3.43	0.10	252.7	262.8	-10.0	0.4	3.31
2339	3.62	0.09	255.1	263.4	-8.3	0.6	3.31
2349	3.75	0.09	251.6	257.8	-6.2	2.6	3.37
2359	3.58	0.09	254.2	261.2	-7.0	2.4	3.33
0 9	3.73	0.09	253.1	257.5	-4.4	1.8	3.37
019	4.10	0.08	305.1	265.6	39.5	34.6	-3.31
029	4.56	0.06	286.8	268.5	18.3	25.3	-3.30
039	5.12	0.05	275.7	265.5	10.2	20.3	3.34
049	5.71	0.04	263.9	274.7	-10.8	1.9	3.27
059	5.57	0.05	264.0	275.8	-11.9	2.8	3.26
1 9	7.80	0.03	266.9	280.6	-13.7	3.1	3.24
119	9.25	0.02	257.5	273.5	-16.0	2.6	3.31
129	9.51	0.02	271.0	281.3	-10.4	2.1	3.25
139	9.25	0.02	279.4	296.6	-17.1	0.5	3.13
149	8.99	0.02	273.2	287.7	-14.4	3.1	3.19
159	8.19	0.02	265.3	265.3	0.0	1.6	-3.37
2 9	8.99	0.02	289.9	305.1	-15.2	3.4	3.07
219	8.46	0.02	283.8	303.7	-19.8	1.0	3.08
229	8.19	0.02	275.3	289.7	-14.4	2.2	3.17
239	8.19	0.02	292.0	312.6	-20.6	1.4	3.02
249	8.72	0.02	306.1	333.4	-27.3	2.3	2.89
259	7.93	0.03	286.3	284.9	1.4	1.1	-3.21
3 9	8.72	0.02	308.2	332.7	-24.4	3.8	2.89
319	7.93	0.03	304.7	286.3	18.4	29.2	-3.20
329	9.25	0.02	328.6	367.0	-38.4	9.4	2.70
339	8.19	0.02	287.1	307.8	-20.7	2.7	3.05
349	7.66	0.03	294.7	290.0	4.7	1.3	-3.17
519	7.40	0.03	320.9	328.4	-7.5	1.7	2.91
619	6.61	0.03	311.8	313.7	-1.8	1.6	3.00
11 9	2.36	0.21	245.5	243.4	2.1	2.9	3.36
1119	2.53	0.18	228.4	207.2	21.2	19.6	-3.79
1129	2.31	0.22	206.7	188.0	18.7	15.9	-4.01
1139	2.41	0.20	214.5	221.6	-7.1	0.7	3.60
1149	2.67	0.16	228.7	231.0	-2.2	2.1	3.54
1159	2.50	0.18	217.8	218.0	-0.1	1.8	3.66
12 9	2.47	0.19	214.0	214.5	-0.5	1.5	3.69
1219	2.30	0.22	223.3	216.3	6.9	1.4	3.63
1229	2.24	0.24	270.4	272.5	-2.1	10.7	3.08
1239	2.45	0.19	254.2	234.3	19.9	18.8	3.47
1249	2.22	0.24	238.2	190.2	47.9	17.8	-3.95
1259	2.28	0.23	221.5	219.6	1.9	1.1	3.59
1329	2.12	0.27	224.3	218.5	5.7	2.2	3.55
1359	1.96	0.33	228.2	206.5	21.7	11.0	3.63

Table 2. Results for Lowell ionograms, showing for each of the ionograms analyzed the values of X = foF2/foE; dM, the correction applied in the Dudeney model to the scaled value of M(3000)F2; the POLAN value of hmF2; the Dudeney value of hmF2; the difference (POLAN - Dudeney) between the two values of hmF2; the standard error in the POLAN value of hmF2; and the value of M(3000)F2. A negative value of M(3000)F2 indicates some uncertainty in the value.

2312	3.13	0.12	226.9	237.2	-10.2	1.8	3.53
2316	3.21	0.11	238.5	235.2	3.3	12.2	3.55
2319	3.57	0.10	274.8	281.4	-6.6	11.6	3.16
2329	2.79	0.15	231.6	229.8	1.9	2.1	3.57
2339	3.15	0.12	264.0	263.8	0.2	13.7	3.28
2349	3.42	0.10	269.2	269.0	0.2	11.3	3.25
2359	3.42	0.10	285.0	274.4	10.6	18.7	-3.21
0 9	3.55	0.10	278.1	257.5	20.6	23.1	-3.36
019	3.90	0.08	274.6	267.9	6.8	17.0	-3.29
029	4.33	0.07	272.9	276.2	-3.2	1.8	3.23
039	4.87	0.06	285.9	284.6	1.2	14.6	3.18
049	5.29	0.05	278.5	277.4	1.1	15.9	3.24
059	5.57	0.05	299.8	315.9	-16.1	24.0	2.97
1 9	7.20	0.03	279.6	301.2	-21.6	3.5	3.09
129	8.99	0.02	290.8	308.3	-17.4	2.8	3.05
149	7.93	0.03	285.6	290.5	-4.9	1.6	3.17
159	8.46	0.02	298.3	326.4	-28.1	2.4	2.93
2 9	8.99	0.02	330.4	346.5	-16.1	3.2	2.81
239	8.19	0.02	323.5	339.2	-15.6	2.0	2.85
249	7.93	0.03	304.0	310.4	-6.4	2.9	-3.03
3 9	8.19	0.02	322.6	339.2	-16.6	3.0	2.85
319	8.19	0.02	308.7	322.3	-13.6	1.0	2.95
329	8.19	0.02	347.6	310.2	37.4	0.4	-3.03
339	8.46	0.02	300.4	317.9	-17.4	3.2	2.98
349	8.46	0.02	315.7	298.2	17.5	31.0	-3.12
359	9.25	0.02	318.6	345.3	-26.7	4.5	2.82
4 9	8.19	0.02	832.3	275.2	557.1	999.0	3.29
429	8.72	0.02	328.8	313.1	15.7	29.0	-3.01
439	8.99	0.02	338.3	314.9	23.4	31.7	-3.00
459	8.46	0.02	276.1	285.4	-9.2	1.9	3.21
5 9	8.72	0.02	300.7	313.8	-13.1	1.3	3.01
539	8.99	0.02	298.8	298.4	0.4	20.3	-3.12
549	8.46	0.02	273.2	278.1	-4.9	1.3	3.27
559	8.72	0.02	303.8	270.4	33.5	39.6	-3.33
6 9	8.99	0.02	298.7	317.3	-18.5	2.0	2.99
619	8.99	0.02	301.3	313.8	-12.5	6.6	3.01
649	7.93	0.03	269.3	262.1	7.3	1.2	-3.40
7 9	8.19	0.02	298.2	329.6	-31.4	2.8	2.91
1129	2.12	0.27	263.1	248.4	14.7	0.6	3.25
1139	2.12	0.27	230.6	235.9	-5.3	4.0	3.37
1149	2.06	0.29	214.4	199.6	14.8	12.8	-3.76
1159	1.94	0.33	209.7	201.5	8.2	8.3	3.68
12 9	2.00	0.31	261.5	238.2	23.2	16.2	-3.30
1219	1.95	0.33	246.0	194.6	51.3	29.8	-3.77
1229	1.90	0.35	256.8	221.6	35.2	1.3	3.42
1239	1.86	0.38	273.7	210.0	63.8	0.4	-3.53
1249	1.91	0.35	237.2	238.0	-0.8	7.2	3.26
1259	1.83	0.40	231.9	219.9	12.0	6.6	3.38
13 9	1.71	0.50	224.5	179.1	45.3	18.6	-3.79
14 9	1.66	0.56	254.1	211.5	42.6	16.6	-3.30
1419	1.33	2.13	209.4	90.2	119.3	12.9	-3.54

Table 2 (Continued)

1429	1.72	0.48	248.1	240.3	7.8	9.0	3.09
1439	1.72	0.48	247.5	217.2	30.3	14.0	-3.32

Table 2 (Continued)

ARGENTIA FEB 1986 Universal Time

TIME	X	dM	POL	DUD	DIFF	STER	M
2149	2.64	0.17	288.7	293.2	-4.5	2.6	3.00
2154	2.80	0.15	267.6	276.0	-8.4	0.8	3.15
2159	2.60	0.17	282.2	264.6	17.6	16.8	-3.21
22 4	3.00	0.13	288.3	304.4	-16.1	2.3	2.96
22 9	3.37	0.11	273.6	310.2	-36.6	6.8	2.94
2214	3.29	0.11	270.8	268.7	2.1	2.6	-3.25
2219	4.00	0.08	264.3	290.3	-26.0	2.1	3.11
2224	3.67	0.09	271.9	306.7	-34.8	3.6	2.98
2231	5.75	0.04	305.7	356.5	-50.8	11.8	2.73
2237	5.06	0.05	281.3	311.0	-29.6	5.2	2.99
2244	5.06	0.05	337.8	383.6	-45.8	16.0	2.59
1019	1.47	0.99	400.0	254.5	145.4	24.9	-2.45
1039	1.50	0.88	209.8	173.5	36.2	8.1	-3.42
1149	1.81	0.41	249.9	220.7	29.2	1.6	3.36
1154	1.68	0.53	212.4	194.7	17.7	0.5	3.54
1159	1.81	0.41	209.1	201.5	7.6	3.4	3.59
12 9	1.77	0.44	206.7	188.8	17.9	2.1	3.72
1214	1.71	0.50	211.9	197.1	14.8	5.1	3.54
1219	1.82	0.41	202.5	201.7	0.8	0.6	3.59
1224	1.82	0.41	229.4	217.4	12.0	10.6	3.41
1229	1.74	0.47	207.9	209.8	-1.9	7.8	3.42
1234	1.83	0.40	214.2	211.4	2.8	2.0	3.48
1239	1.83	0.40	208.3	213.2	-4.9	2.6	3.46
1244	1.83	0.40	210.2	207.8	2.4	2.2	3.52
1249	1.83	0.40	211.0	208.8	2.1	0.7	3.51
1254	1.83	0.40	210.5	208.8	1.6	0.9	3.51
1259	1.65	0.56	213.4	199.7	13.7	3.6	3.43
13 4	1.62	0.62	208.5	189.6	18.8	1.9	3.50
13 9	1.62	0.62	206.2	186.3	19.8	1.3	3.54
1319	1.58	0.69	208.8	183.8	25.0	2.9	3.50
1324	1.62	0.62	214.3	192.8	21.5	4.2	3.45
1329	1.65	0.56	204.7	203.6	1.1	13.1	-3.38
1334	1.65	0.56	239.3	217.1	22.2	2.1	3.23
1339	1.69	0.52	251.1	217.7	33.3	4.5	3.28
1344	1.69	0.52	250.9	225.3	25.5	16.6	3.20
1349	1.63	0.60	243.7	209.8	33.9	13.0	3.28
1354	1.63	0.60	207.7	209.3	-1.6	12.4	3.28
1359	1.63	0.60	204.8	204.7	0.1	11.3	3.33
1424	1.67	0.55	220.7	202.8	18.0	2.8	3.41
1429	1.57	0.70	217.7	191.2	26.5	8.4	3.38
1434	1.69	0.52	224.5	204.8	19.7	2.3	3.42
1439	1.63	0.60	218.1	193.7	24.3	1.3	3.47
1444	1.64	0.58	210.7	202.0	8.7	12.9	3.39
1449	1.64	0.58	209.0	192.2	16.8	3.7	3.51
1454	1.61	0.63	210.3	188.8	21.5	6.6	3.49
1459	1.67	0.55	236.5	211.7	24.8	2.1	3.31
15 4	1.57	0.70	213.9	188.7	25.2	3.3	3.42

Table 3. Results for Argentia ionograms, showing for each of the ionograms analyzed the values of X = foF2/foE; dM, the correction applied in the Dudeney model to the scaled value of M(3000)F2; the POLAN value of hmF2; the Dudeney value of hmF2; the difference (POLAN - Dudeney) between the two values of hmF2; the standard error in the POLAN value of hmF2; and the value of M(3000)F2. A negative value of M(3000)F2 indicates some uncertainty in the value.

15 9	1.57	0.70	205.8	186.5	19.3	6.1	3.45
1514	1.70	0.51	229.1	214.6	14.5	6.9	3.33
1519	1.64	0.58	219.3	208.0	11.4	10.4	3.32
1524	1.71	0.49	256.2	240.5	15.7	14.1	3.07
1529	1.70	0.51	222.8	215.0	7.8	9.4	3.32
1534	1.66	0.56	229.4	217.9	11.5	8.9	3.22
1539	1.79	0.43	239.9	227.1	12.8	5.3	3.28
1544	1.75	0.46	230.3	219.3	11.0	3.7	3.33
16 4	1.81	0.41	220.7	215.8	4.9	4.4	3.42
1614	1.71	0.49	223.4	212.4	11.0	5.4	3.36
1619	1.75	0.46	225.8	220.5	5.3	2.8	3.31
1624	1.69	0.52	213.6	202.9	10.7	3.3	3.44
1629	1.75	0.46	220.3	210.0	10.3	4.4	3.43
1634	1.75	0.46	217.3	210.0	7.3	3.8	3.43
1639	1.71	0.49	206.4	195.2	11.2	4.6	3.57
1644	1.75	0.46	221.1	214.9	6.2	0.8	3.37
1649	1.64	0.58	203.3	191.8	11.5	8.3	3.52
1654	1.68	0.53	209.7	206.2	3.4	7.2	3.39
17 9	1.70	0.51	208.6	192.8	15.8	11.5	-3.59
1729	1.81	0.41	245.2	229.8	15.3	16.3	3.27
1734	1.70	0.51	204.9	199.0	5.9	6.8	3.51
18 4	1.85	0.39	227.9	226.9	0.9	2.1	3.33
1839	2.00	0.31	261.9	230.0	31.9	1.2	3.38
1859	2.04	0.29	229.7	219.6	10.1	1.4	3.51
19 9	2.13	0.26	242.3	224.6	17.7	3.0	3.49
1914	2.13	0.26	234.8	229.3	5.6	1.2	3.44
1919	2.18	0.25	246.4	227.5	18.9	1.7	3.48
1924	2.23	0.24	253.1	239.3	13.8	6.4	3.37
1929	2.18	0.25	235.7	230.2	5.5	1.2	3.45
1934	2.24	0.24	233.2	231.7	1.5	1.1	3.45
1939	2.29	0.22	240.0	239.0	1.0	1.2	3.39
1944	2.19	0.25	230.0	223.1	6.9	1.3	3.53
1949	2.35	0.21	246.8	240.4	6.4	2.4	3.39
1954	2.35	0.21	250.0	243.9	6.1	3.0	3.36
1959	2.20	0.24	229.4	220.0	9.3	1.4	3.57
20 4	2.32	0.22	226.4	224.2	2.2	1.5	3.55
20 9	2.32	0.22	227.2	226.3	0.9	2.0	3.53
2014	2.21	0.24	230.5	225.9	4.6	1.6	3.50
2019	2.33	0.21	235.0	237.9	-2.8	2.4	3.41
2024	2.33	0.21	246.9	245.0	1.9	3.1	3.34
2029	2.28	0.23	251.1	246.2	4.9	3.1	3.32
2034	2.35	0.21	237.0	229.8	7.2	0.9	3.50
2039	2.35	0.21	237.5	235.3	2.3	1.1	3.44
2044	2.35	0.21	254.6	252.9	1.7	3.0	3.27
2049	2.37	0.21	245.2	244.7	0.4	1.1	3.35
2054	2.37	0.21	261.8	259.0	2.8	3.0	3.22
2059	2.31	0.22	243.5	242.8	0.7	0.7	3.36
21 4	2.53	0.18	244.1	243.9	0.2	1.7	3.39
2114	1.94	0.33	243.8	241.8	2.0	1.0	3.24
2119	2.43	0.20	245.7	242.9	2.8	2.1	3.38
2124	2.77	0.15	263.4	267.7	-4.3	3.1	3.21

Table 3 (Continued)

2129	2.62	0.17	281.8	286.6	-4.8	2.4	3.04
2134	2.92	0.14	302.8	312.8	-10.0	1.3	2.89
2139	2.75	0.15	284.1	290.6	-6.5	3.0	3.03
2144	3.00	0.13	289.5	299.1	-9.6	2.4	2.99
2149	3.00	0.13	275.7	248.7	27.0	29.8	-3.40
2154	3.70	0.09	312.0	323.9	-11.9	2.1	2.87
2159	3.20	0.12	265.8	277.0	-11.2	0.6	3.17
22 4	3.67	0.09	281.2	297.9	-16.7	1.1	3.04
22 9	4.12	0.07	298.7	315.7	-17.0	2.2	2.94
2214	4.71	0.06	305.9	324.6	-18.6	2.2	2.90
2219	5.17	0.05	264.5	272.2	-7.7	2.0	3.28
2224	5.50	0.05	302.3	323.0	-20.8	3.2	2.92
2229	6.00	0.04	278.4	296.2	-17.8	0.6	3.11
2234	8.25	0.02	325.5	350.8	-25.3	2.0	2.79
2239	8.36	0.02	334.1	355.8	-21.8	2.0	2.76
2244	7.60	0.03	294.9	309.7	-14.8	0.5	3.03
2249	7.85	0.03	296.6	306.8	-10.1	0.7	3.05
2254	7.34	0.03	300.1	317.4	-17.3	3.0	2.98
2259	7.60	0.03	296.2	315.2	-19.0	3.1	2.99
23 4	7.34	0.03	308.1	324.9	-16.7	2.2	2.93
23 9	7.09	0.03	301.5	314.4	-12.9	0.6	2.99
2314	7.60	0.03	325.4	350.7	-25.3	3.3	2.78
2319	7.09	0.03	295.6	312.9	-17.3	0.5	3.01
2324	7.09	0.03	311.3	328.2	-16.9	4.6	2.91
2329	7.09	0.03	319.1	340.2	-21.2	4.2	2.84
2334	6.84	0.03	299.2	311.8	-12.5	0.5	3.01
2339	5.82	0.04	296.8	269.5	27.3	33.4	-3.32
2344	6.58	0.04	321.5	342.1	-20.6	1.8	2.82
2349	6.33	0.04	327.7	353.4	-25.7	4.5	2.76
2354	6.08	0.04	296.0	318.4	-22.3	1.7	2.96
2359	6.58	0.04	276.3	282.1	-5.7	1.0	3.22
0 4	6.58	0.04	276.1	289.4	-13.3	0.7	3.17
0 9	6.08	0.04	280.0	293.9	-13.9	0.4	3.13
014	6.84	0.03	287.6	304.6	-16.9	0.8	3.06
019	6.84	0.03	298.0	319.9	-21.9	4.7	2.96
024	6.84	0.03	291.2	309.2	-18.0	1.5	3.03
029	5.82	0.04	276.4	289.9	-13.6	0.4	3.15
034	6.08	0.04	277.0	289.4	-12.5	0.7	3.16
039	6.58	0.04	288.1	304.1	-15.9	0.6	3.06
044	5.82	0.04	275.5	289.9	-14.5	0.4	3.15
049	6.58	0.04	293.8	306.2	-12.4	1.6	3.05
054	5.57	0.05	271.2	284.6	-13.4	0.7	3.19
059	6.08	0.04	291.3	307.1	-15.8	0.5	3.03
1 4	6.08	0.04	290.9	307.1	-16.2	0.5	3.03
1 9	6.08	0.04	294.2	316.8	-22.6	1.1	2.97
114	5.82	0.04	290.3	312.9	-22.6	1.0	2.99
119	6.08	0.04	338.4	361.9	-23.5	4.3	2.71
124	6.08	0.04	327.0	353.6	-26.6	4.0	2.75
129	6.08	0.04	312.2	332.6	-20.4	1.3	2.87
134	5.57	0.05	315.5	332.2	-16.6	1.9	2.87
139	5.82	0.04	350.8	382.3	-31.5	2.7	2.61

Table 3 (Continued)

144	5.57	0.05	312.1	343.4	-31.3	2.7	2.80
149	6.08	0.04	366.1	395.0	-28.9	2.0	2.55
154	5.32	0.05	313.3	337.6	-24.3	2.9	2.83
159	5.32	0.05	311.1	330.1	-19.1	2.2	2.88
2 4	5.57	0.05	323.5	341.8	-18.4	2.8	2.81
2 9	4.81	0.06	300.7	276.1	24.6	18.1	-3.24
214	5.06	0.05	305.9	320.7	-14.8	1.5	2.93
219	5.32	0.05	322.6	357.0	-34.4	3.7	2.73
224	5.57	0.05	366.4	400.0	-33.6	1.6	2.52
229	5.06	0.05	353.4	375.8	-22.4	3.8	2.63
234	4.81	0.06	343.8	400.3	-56.5	12.0	2.51
239	5.06	0.05	350.7	371.5	-20.8	4.3	2.65
244	4.81	0.06	345.0	370.5	-25.6	4.7	2.65
249	5.06	0.05	338.0	361.8	-23.7	3.9	2.70
254	4.81	0.06	303.7	318.9	-15.2	1.6	2.94
259	4.30	0.07	326.6	361.6	-34.9	1.1	2.68
3 9	4.81	0.06	373.7	413.8	-40.2	6.5	2.45
314	4.81	0.06	331.2	372.8	-41.5	6.0	2.64
319	4.30	0.07	307.4	340.6	-33.2	1.3	2.80
324	4.30	0.07	298.5	328.8	-30.3	1.2	2.86
329	4.30	0.07	333.6	342.5	-8.9	0.7	2.78
334	4.56	0.06	331.5	360.8	-29.2	2.5	2.69
429	4.81	0.06	328.8	403.7	-74.9	21.2	2.50
444	4.05	0.08	303.2	341.5	-38.3	3.3	2.78
449	4.30	0.07	306.5	350.1	-43.6	5.0	2.74
514	4.30	0.07	313.6	357.7	-44.1	6.8	2.70
1039	1.62	0.61	225.3	199.6	25.7	1.2	3.39
1044	1.65	0.57	217.8	194.6	23.3	0.4	3.49
1049	1.76	0.45	217.5	210.7	6.8	1.6	3.43
1054	1.82	0.40	216.1	210.2	5.9	4.5	3.49
11 9	1.89	0.36	221.5	215.8	5.7	0.6	3.48
1114	1.90	0.36	223.4	219.9	3.5	0.4	3.44
1119	1.95	0.33	223.0	219.6	3.4	0.7	3.47
1124	2.11	0.27	221.1	218.3	2.8	1.1	3.55
1129	2.21	0.24	220.6	224.8	-4.2	3.6	3.52
1134	1.90	0.35	212.2	209.9	2.3	4.0	3.55
1139	1.86	0.38	214.2	208.8	5.4	0.4	3.54
1144	1.95	0.33	229.9	234.0	-4.1	2.4	3.32
1149	1.86	0.38	234.3	227.5	6.7	2.4	3.33
1154	2.00	0.31	227.8	225.9	1.9	0.4	3.43
1159	1.86	0.38	226.2	201.0	25.2	14.2	-3.63
12 4	2.00	0.31	225.3	221.1	4.1	0.7	3.48
1214	2.05	0.29	222.4	214.7	7.6	1.6	3.57
1219	2.09	0.28	232.8	232.4	0.4	1.6	3.40
1224	2.00	0.31	228.3	223.0	5.3	3.0	3.46
1229	1.96	0.33	220.2	211.5	8.7	1.1	3.57
1234	2.00	0.31	213.0	212.2	0.7	2.0	3.58
1239	2.00	0.31	215.9	208.9	7.0	1.3	3.62
1244	1.96	0.33	213.0	207.7	5.3	1.4	3.61
1249	2.00	0.31	231.7	232.4	-0.7	2.3	3.36
1254	1.92	0.35	212.0	213.3	-1.2	0.6	3.52

Table 3 (Continued)

1259	1.85	0.39	223.0	222.2	0.8	2.0	3.37
13 4	1.88	0.37	217.7	208.2	9.5	0.9	3.56
13 9	1.87	0.37	211.5	181.6	30.0	18.3	-3.91
1314	1.85	0.39	209.1	191.1	18.0	10.8	-3.75
1319	1.88	0.37	212.5	203.2	9.3	8.8	-3.62
1324	1.77	0.44	200.1	192.0	8.1	1.5	3.67
1329	1.77	0.44	204.2	190.8	13.3	1.7	3.69
1334	1.81	0.41	225.8	214.7	11.1	6.2	3.43
1339	1.67	0.55	209.6	203.8	5.8	3.5	3.40
1344	1.81	0.41	212.0	204.3	7.7	0.6	3.56
1349	1.81	0.41	208.6	201.9	6.7	1.1	3.59
1354	1.78	0.44	214.0	208.9	5.1	3.9	3.47
1359	1.74	0.47	210.0	202.9	7.1	4.0	3.51
14 4	1.70	0.51	221.3	208.4	12.9	5.3	3.40
14 9	1.85	0.39	229.6	229.8	-0.2	1.7	3.30
1414	1.78	0.44	220.8	226.8	-6.0	11.9	3.87
1419	1.93	0.34	246.4	249.7	-3.2	0.9	3.15
1424	1.93	0.34	258.8	254.0	4.7	5.1	3.12
1429	1.89	0.36	235.2	238.3	-3.1	2.6	3.24
1434	1.89	0.36	232.8	238.3	-5.5	3.3	3.24
1439	1.89	0.36	235.0	239.5	-4.5	2.8	3.23
1444	1.93	0.34	240.0	236.9	3.1	8.1	3.28
1449	2.04	0.30	262.8	264.8	-2.0	1.9	3.08
1454	1.96	0.33	236.9	238.9	-2.0	3.8	3.28
1459	1.76	0.45	230.8	204.5	26.3	16.3	-3.50
15 4	2.04	0.30	246.8	242.0	4.7	1.2	3.28
15 9	1.78	0.44	216.6	181.9	34.7	20.5	-3.82
1514	1.86	0.38	219.4	212.7	6.7	3.3	3.49
1519	1.83	0.40	220.8	211.6	9.2	0.4	3.48
1524	1.79	0.43	212.6	207.9	4.8	0.5	3.49
1529	1.93	0.34	224.4	224.2	0.2	4.4	3.40
1534	2.00	0.31	224.1	221.4	2.7	0.8	3.47
1539	1.93	0.34	225.1	221.9	3.3	0.4	3.43
1544	1.83	0.40	212.8	206.0	6.9	2.4	3.55
1549	2.00	0.31	209.7	208.7	0.9	1.0	3.62
1554	1.96	0.33	217.3	217.3	0.0	3.1	3.50
1559	1.86	0.38	231.2	208.1	23.1	14.0	-3.55
16 4	2.04	0.30	232.3	209.3	23.0	17.6	-3.63
16 9	1.55	0.75	199.7	159.5	40.2	14.4	-3.79
1614	2.07	0.28	218.2	213.9	4.3	0.9	3.59
1619	2.22	0.24	228.9	220.7	8.2	1.6	3.57
1624	1.93	0.34	212.6	207.0	5.6	0.2	3.61
1629	2.00	0.31	217.3	212.5	4.8	1.2	3.58
1634	2.22	0.24	220.1	217.2	3.0	0.8	3.60
1639	2.19	0.25	218.6	218.8	-0.3	1.4	3.57
1644	2.00	0.31	227.9	198.9	29.0	19.5	-3.74
1649	2.07	0.28	214.9	217.1	-2.1	1.6	3.55
1654	2.00	0.31	221.0	216.7	4.3	1.2	3.53
1659	2.29	0.22	238.9	243.3	-4.5	4.1	3.35
17 4	1.96	0.33	232.6	238.4	-5.8	5.3	3.28
17 9	1.86	0.38	225.6	234.7	-9.1	7.4	3.25

Table 3 (Continued)

1714	1.93	0.34	233.5	238.4	-5.0	3.7	3.26
1719	1.86	0.38	245.8	246.3	-0.5	2.7	3.14
1724	1.93	0.34	245.9	258.4	-12.5	9.0	3.08
1729	2.08	0.28	262.0	272.5	-10.5	3.1	3.03
1734	2.15	0.26	263.4	268.6	-5.2	1.8	3.09
1739	2.19	0.25	299.3	302.6	-3.3	5.6	2.85
1744	2.15	0.26	274.9	282.3	-7.4	1.9	2.98
1749	2.23	0.24	286.6	288.2	-1.6	2.4	2.96
1759	2.19	0.25	260.5	259.1	1.3	0.7	3.18
1814	2.22	0.24	279.6	271.3	8.3	5.8	3.09
1819	2.31	0.22	269.9	265.1	4.8	1.3	3.16
1824	2.58	0.17	262.9	264.2	-1.3	0.4	3.22
1849	2.68	0.16	243.4	244.5	-1.1	2.0	3.41
1854	2.57	0.18	249.5	247.0	2.5	1.4	3.37
19 4	2.52	0.18	259.4	261.0	-1.6	5.9	3.23
1944	2.76	0.15	265.8	271.3	-5.4	0.9	3.18
1949	2.76	0.15	267.2	271.5	-4.3	1.6	3.18
1954	2.85	0.14	259.1	256.1	2.9	2.9	3.32
20 4	3.50	0.10	265.6	274.4	-8.8	0.5	3.21
20 9	2.67	0.16	261.9	264.5	-2.7	1.4	3.22
2013	3.22	0.11	296.3	300.9	-4.6	4.6	3.00
2029	2.87	0.14	242.5	226.0	16.6	0.4	3.62
2034	3.47	0.10	288.4	286.3	2.2	1.0	3.12
2049	3.75	0.09	269.0	269.0	0.0	0.6	3.27
21 4	3.93	0.08	260.3	264.7	-4.4	1.9	3.31
2114	4.14	0.07	257.0	260.9	-3.9	1.3	3.35
2124	4.31	0.07	257.1	262.9	-5.8	2.8	3.34
2129	4.15	0.07	257.7	263.8	-6.0	2.8	3.33
2134	4.25	0.07	261.3	263.6	-2.3	2.0	3.33
2139	3.92	0.08	265.8	273.6	-7.9	1.1	3.24
2144	3.73	0.09	242.7	252.2	-9.5	1.0	3.42
2149	3.64	0.09	267.3	278.6	-11.3	1.1	3.19
2154	4.00	0.08	290.0	307.8	-17.9	3.2	2.99
2159	3.80	0.09	316.4	333.5	-17.1	5.2	2.82
22 4	4.22	0.07	334.1	359.3	-25.2	8.9	2.69
22 9	4.75	0.06	347.9	373.6	-25.7	8.7	2.63
2214	5.43	0.05	334.5	355.0	-20.5	3.4	2.74
2219	6.50	0.04	350.5	370.6	-20.1	4.7	2.67
2224	6.33	0.04	347.1	371.8	-24.6	4.3	2.66
2229	6.20	0.04	290.3	307.0	-16.6	0.8	3.04
2234	8.00	0.03	301.6	321.1	-19.5	1.5	2.96
2239	8.86	0.02	329.5	357.4	-27.9	5.5	2.75
2244	8.86	0.02	324.8	347.2	-22.4	2.6	2.81
2249	8.10	0.02	326.9	354.3	-27.4	3.4	2.77
2254	7.60	0.03	306.2	325.7	-19.5	1.9	2.93
2259	7.60	0.03	329.0	357.1	-28.2	3.9	2.75
23 4	7.85	0.03	347.2	374.9	-27.7	3.3	2.66
23 9	6.84	0.03	300.6	317.6	-17.0	1.3	2.97
2314	7.85	0.03	361.2	385.3	-24.1	4.1	2.61
2319	7.34	0.03	312.2	335.3	-23.1	1.2	2.87
2324	8.10	0.02	329.0	352.7	-23.7	1.2	2.77

Table 3 (Continued)

2329	5.82	0.04	266.4	273.0	-6.5	1.7	-3.29
2334	6.33	0.04	277.5	280.6	-3.1	1.6	-3.23
2339	7.85	0.03	355.1	377.4	-22.3	2.5	2.65
2344	6.84	0.03	299.9	319.8	-19.9	1.4	2.96
2349	7.34	0.03	343.6	356.7	-13.1	3.9	2.75
2354	7.09	0.03	322.7	347.5	-24.8	0.7	2.80
2359	7.34	0.03	346.5	354.1	-7.6	4.6	2.76
0 4	7.60	0.03	366.2	400.0	-33.8	8.2	2.54
0 9	5.82	0.04	280.1	297.4	-17.2	2.0	3.10
014	5.82	0.04	289.9	308.4	-18.6	0.8	3.02
019	5.32	0.05	273.6	290.6	-17.0	0.3	3.14
024	6.84	0.03	346.0	367.6	-21.6	2.2	2.69
029	6.33	0.04	336.3	351.7	-15.4	5.0	2.77
034	6.08	0.04	326.7	356.2	-29.4	3.0	2.74
039	5.82	0.04	308.0	315.8	-7.9	0.4	2.97
044	5.82	0.04	364.1	395.1	-31.1	1.9	2.55
049	5.57	0.05	390.7	344.1	46.6	17.2	-2.80
054	5.82	0.04	409.6	403.7	5.8	3.7	2.51
1 4	4.30	0.07	336.0	386.8	-50.8	8.4	2.56
1 9	4.30	0.07	369.4	429.1	-59.7	9.2	2.38
114	4.56	0.06	324.6	343.8	-19.2	3.8	2.78
119	4.30	0.07	317.7	346.3	-28.6	1.1	2.76
124	5.06	0.05	382.9	480.3	-97.4	21.0	2.22
134	5.06	0.05	383.1	448.0	-64.9	14.5	-2.33
139	4.56	0.06	363.0	404.7	-41.7	4.2	2.49
144	3.80	0.09	328.4	357.8	-29.3	0.6	2.68
149	4.05	0.08	357.6	390.2	-32.6	3.7	2.54
159	4.56	0.06	429.6	466.9	-37.3	8.5	2.25
2 9	5.06	0.05	472.4	484.8	-12.4	23.9	-2.20
244	5.06	0.05	380.8	390.6	-9.9	4.6	-2.56
249	5.57	0.05	404.4	452.7	-48.3	12.7	2.32
254	5.32	0.05	910.4	510.3	400.1	999.0	2.13
259	5.57	0.05	367.5	380.6	-13.1	3.4	2.61
3 4	4.56	0.06	336.5	326.0	10.5	37.3	-2.89
314	6.58	0.04	278.0	231.5	46.5	22.8	-3.68
339	6.08	0.04	177.2	189.3	-12.1	-4.8	4.21
349	5.82	0.04	503.4	443.0	60.5	-0.1	2.36
4 4	5.57	0.05	503.9	439.6	64.3	0.9	-2.37
419	5.32	0.05	198.6	214.1	-15.5	0.8	3.87
434	5.82	0.04	186.6	179.3	7.3	0.2	-4.36
439	6.33	0.04	391.1	440.7	-49.6	12.6	2.37
454	5.32	0.05	360.4	330.7	29.7	39.6	-2.87
459	5.32	0.05	379.0	424.1	-45.1	10.0	2.42
5 4	5.57	0.05	1206.5	463.2	743.3	999.0	2.28

Table 3 (Continued)

GOOSE BAY JAN 1986 Local Time

TIME	X	dM	POL	DUD	DIFF	STER	M
1014	1.96	0.33	213.2	205.0	8.2	1.0	3.64
1029	1.83	0.40	217.9	208.5	9.4	0.5	3.52
1059	1.88	0.37	240.1	215.7	24.5	3.5	3.47
1314	1.88	0.37	244.6	226.8	17.8	0.8	3.35
1329	2.00	0.31	257.8	223.7	34.1	1.1	3.45
1344	2.17	0.25	370.2	230.0	140.2	40.2	3.45
1359	2.12	0.27	231.9	222.7	9.2	0.9	3.51
1414	2.35	0.21	269.6	264.1	5.5	2.4	3.17
1429	2.27	0.23	222.0	208.1	13.9	0.3	3.73
1444	2.23	0.24	222.6	214.9	7.7	1.1	3.63
1459	2.24	0.24	223.7	220.4	3.4	1.3	3.57
1514	2.35	0.21	222.0	223.6	-1.6	1.2	3.57
1529	2.32	0.22	243.6	205.6	38.0	12.5	3.77
1559	2.81	0.15	244.0	263.8	-19.8	4.1	3.25
1614	3.13	0.12	271.0	278.3	-7.3	0.9	3.16
1629	3.21	0.11	240.9	254.2	-13.3	2.4	3.37
1644	3.29	0.11	267.7	273.3	-5.7	1.0	3.21
1659	9.74	0.02	240.0	257.7	-17.7	1.8	3.45
1714	9.74	0.02	254.9	274.5	-19.6	0.9	3.30
1729	9.49	0.02	280.0	285.8	-5.8	3.0	3.21
1744	9.01	0.02	258.8	278.6	-19.7	1.2	3.27
1759	8.76	0.02	259.2	277.4	-18.2	1.0	3.27
1814	8.52	0.02	287.6	303.3	-15.8	4.4	3.08
1829	7.30	0.03	241.0	259.0	-18.0	1.0	3.42
1844	6.82	0.03	254.6	274.8	-20.2	1.0	3.28
1859	6.57	0.04	262.2	284.9	-22.7	0.8	3.20
1914	6.57	0.04	278.8	305.6	-26.8	3.1	3.05
1929	6.57	0.04	307.3	338.4	-31.1	1.9	2.84
1944	6.09	0.04	278.9	311.1	-32.2	2.2	3.01
1959	5.36	0.05	272.5	299.0	-26.5	3.0	3.08
2014	5.36	0.05	287.2	277.8	9.4	0.8	3.24
2029	5.11	0.05	259.5	266.4	-6.9	2.1	3.33
014	7.30	0.03	393.8	327.7	66.0	33.3	2.91
044	7.55	0.03	274.1	208.3	65.8	40.2	3.97
059	13.39	0.01	246.2	201.4	44.8	21.5	4.08
744	1.71	0.49	245.4	205.4	40.0	13.9	3.44
759	2.21	0.24	237.8	251.2	-13.4	1.7	3.26
844	2.33	0.21	232.7	223.4	9.3	1.1	3.56
944	2.33	0.21	242.7	243.2	-0.5	2.5	3.36
1029	2.04	0.29	221.3	209.0	12.2	1.0	3.63
1114	2.17	0.25	209.2	214.2	-5.0	0.9	3.62
1116	2.08	0.28	212.5	212.1	0.4	0.8	3.62
1121	1.75	0.46	211.8	191.6	20.2	0.6	3.66
1129	1.88	0.37	213.3	204.2	9.0	0.4	3.61
1144	2.61	0.17	273.5	273.9	-0.4	14.6	3.14
1159	1.96	0.33	212.0	201.0	11.0	3.2	3.70
1214	1.88	0.37	220.6	212.2	8.5	3.5	3.51

Table 4. Results for Goose Bay ionograms, showing for each of the ionograms analyzed the values of X = foF2/foE; dM, the correction applied in the Dudeney model to the scaled value of M(3000)F2; the POLAN value of hmF2; the Dudeney value of hmF2; the difference (POLAN - Dudeney) between the two values of hmF2; the standard error in the POLAN value of hmF2; and the value of M(3000)F2. A negative value of M(3000)F2 indicates some uncertainty in the value.

1229	2.04	0.30	240.9	209.0	31.9	0.7	3.63
1314	2.12	0.27	246.6	236.4	10.2	0.3	3.37
1359	2.27	0.23	221.1	221.4	-0.4	0.8	3.57
1414	2.43	0.20	234.8	238.3	-3.6	1.0	3.43
1429	2.67	0.16	282.2	277.2	5.0	7.7	3.12
1444	2.36	0.21	240.5	236.4	4.1	1.1	3.43
1544	2.88	0.14	246.5	245.7	0.8	2.2	3.42
1559	3.00	0.13	239.5	242.4	-2.8	1.3	3.46
1614	3.13	0.12	238.1	243.5	-5.4	1.0	3.46
1629	3.29	0.11	251.4	254.7	-3.2	1.2	3.37
1644	3.21	0.11	259.6	265.6	-6.1	1.0	3.27
1659	10.71	0.01	266.9	290.4	-23.5	1.0	3.18
1714	10.71	0.01	285.1	306.8	-21.6	2.2	3.06
1729	10.96	0.01	277.2	294.2	-17.0	4.3	3.15
1744	10.23	0.02	267.3	294.2	-26.9	1.1	3.15
1759	9.49	0.02	236.3	254.5	-18.2	0.9	3.47
1814	8.28	0.02	243.1	262.4	-19.3	0.6	3.40
1829	8.03	0.03	289.5	316.1	-26.6	2.1	2.99
1844	7.30	0.03	270.2	298.1	-27.9	1.2	3.11
1859	6.57	0.04	283.6	310.5	-27.0	2.0	3.02
1914	6.57	0.04	320.3	334.8	-14.5	5.0	2.86
1929	6.09	0.04	287.2	314.2	-27.1	1.6	2.99
1944	5.36	0.05	264.5	268.5	-4.1	0.9	3.32
1959	5.36	0.05	283.9	288.6	-4.7	0.5	3.16
2014	5.84	0.04	338.8	398.0	-59.2	26.5	2.54

Table 4 (Continued)

RICHFIELD SEP 1984 Universal Time

TIME	X	dM	POL	DUD	DIFF	STER	M
1659	2.43	0.20	248.7	257.2	-8.5	0.5	3.25
1759	2.47	0.19	245.6	245.0	0.6	6.0	3.37
1859	2.32	0.22	272.2	273.3	-1.1	0.9	3.09
1959	2.93	0.14	267.3	266.5	0.8	10.0	3.24
20 9	2.68	0.16	253.8	253.7	0.2	2.4	3.32
2019	3.04	0.13	270.4	266.4	4.0	1.9	3.25
2029	3.07	0.12	283.7	284.6	-0.9	13.2	3.11
2039	2.93	0.14	256.3	265.2	-8.9	1.0	3.25
2044	3.16	0.12	256.0	265.4	-9.4	1.1	3.27
2049	2.82	0.15	257.7	263.6	-5.9	5.7	3.25
2054	3.08	0.12	254.1	264.1	-10.0	2.5	3.27
2059	3.08	0.12	256.0	268.3	-12.3	5.2	3.24
21 4	2.66	0.16	256.9	263.7	-6.8	4.2	3.23
21 9	2.66	0.16	259.1	265.8	-6.7	2.9	3.21
2114	2.66	0.16	260.8	265.0	-4.2	3.1	3.22
2119	2.79	0.15	266.3	270.6	-4.3	3.0	3.19
2124	2.71	0.16	266.5	260.3	6.2	10.9	3.27
2129	2.79	0.15	257.8	265.4	-7.6	0.5	3.23
2134	2.79	0.15	254.9	258.4	-3.5	2.5	3.29
2139	2.89	0.14	256.3	262.4	-6.1	0.8	3.27
2144	2.89	0.14	255.7	267.7	-12.1	2.9	3.22
2149	2.85	0.14	254.2	258.9	-4.7	2.4	3.30
2154	2.85	0.14	260.9	258.2	2.7	7.4	3.30
2159	2.81	0.15	255.9	257.7	-1.8	1.9	3.30
22 4	3.04	0.13	257.4	263.3	-5.9	2.2	3.28
22 9	3.04	0.13	255.9	260.7	-4.7	0.4	3.30
2214	2.74	0.15	246.6	245.7	0.8	0.9	3.40
2219	3.04	0.13	257.4	256.9	0.5	2.1	3.33
2224	3.17	0.12	251.6	255.5	-3.9	0.9	3.35
2229	3.12	0.12	262.1	250.3	11.8	14.7	3.40
2234	3.30	0.11	253.6	258.4	-4.7	0.7	3.34
2239	3.12	0.12	246.7	252.6	-5.9	1.3	3.38
2244	3.00	0.13	250.1	247.4	2.7	7.4	3.41
2249	2.96	0.13	240.5	243.9	-3.5	1.3	3.44
2254	2.96	0.13	239.9	245.2	-5.3	2.3	3.43
2259	2.76	0.15	244.3	248.8	-4.5	5.8	3.38
23 4	3.55	0.10	267.4	274.3	-6.9	8.7	3.22
23 9	2.83	0.14	245.5	253.5	-8.0	3.1	3.34
2314	2.00	0.31	215.8	183.0	32.8	24.6	-3.96
2319	3.29	0.11	257.2	268.0	-10.7	3.0	3.25
2324	2.96	0.13	252.2	258.3	-6.1	2.4	3.31
2329	4.25	0.07	258.5	257.4	1.1	13.5	3.39
2334	4.17	0.07	300.1	289.1	11.0	12.8	3.13
2339	5.00	0.05	240.4	251.0	-10.6	1.2	3.47
2344	3.94	0.08	258.0	252.2	5.8	1.8	3.42
2349	4.37	0.07	265.0	245.5	19.6	1.2	3.50
2354	4.25	0.07	235.2	241.9	-6.7	1.4	3.54

Table 5. Results for Richfield ionograms, showing for each of the ionograms analyzed the values of X = foF2/foE; dM, the correction applied in the Dudeney model to the scaled value of M(3000)F2; the POLAN value of hmF2; the Dudeney value of hmF2; the difference (POLAN - Dudeney) between the two values of hmF2; the standard error in the POLAN value of hmF2; and the value of M(3000)F2. A negative value of M(3000)F2 indicates some uncertainty in the value.

2359	2.44	0.19	222.5	173.4	49.0	25.6	-4.26
014	2.87	0.14	203.6	187.7	15.9	0.3	4.11
019	4.21	0.07	245.0	230.9	14.1	15.7	3.65
024	4.29	0.07	252.5	257.9	-5.4	1.4	3.38
029	4.07	0.08	267.6	254.9	12.6	15.3	3.40
034	4.92	0.06	298.1	301.7	-3.6	17.5	3.05
039	4.31	0.07	248.0	253.9	-6.0	0.7	3.42
044	4.31	0.07	259.1	268.1	-9.0	0.5	3.30
049	4.50	0.07	260.9	263.7	-2.8	9.7	3.34
054	4.58	0.06	258.7	268.9	-10.3	1.0	3.30
059	4.58	0.06	262.3	278.5	-16.1	3.8	3.22
1 4	5.00	0.05	271.5	288.6	-17.1	1.1	3.15
1 9	5.09	0.05	291.4	295.9	-4.5	4.9	3.10
114	5.60	0.05	270.8	276.2	-5.3	1.6	3.26
119	6.00	0.04	274.1	282.5	-8.4	0.7	3.21
124	7.00	0.03	278.8	285.4	-6.5	1.3	3.20
129	6.56	0.04	252.2	255.2	-3.0	0.7	3.45
134	7.50	0.03	250.2	258.3	-8.1	1.3	3.43
139	7.50	0.03	250.7	261.5	-10.8	0.9	3.40
144	8.29	0.02	244.0	253.7	-9.8	1.3	3.48
149	8.43	0.02	251.6	266.3	-14.7	3.8	3.36
154	9.83	0.02	268.9	272.7	-3.9	8.7	3.32
159	9.33	0.02	263.9	265.0	-1.1	7.7	3.38
2 4	10.60	0.01	240.6	253.0	-12.4	1.8	3.49
2 9	9.60	0.02	221.5	228.8	-7.3	1.3	3.73
859	7.60	0.03	302.7	317.5	-14.7	0.7	2.98
959	7.85	0.03	335.2	342.6	-7.5	1.1	2.83
1059	8.36	0.02	328.8	346.7	-17.9	2.4	2.81
1159	4.25	0.07	274.3	279.1	-4.8	0.7	3.20
1259	2.92	0.14	256.6	260.8	-4.2	3.6	3.29
1359	2.87	0.14	229.1	228.3	0.8	1.6	3.60
1459	2.68	0.16	241.9	245.4	-3.5	3.0	3.40
1559	2.96	0.13	232.3	235.3	-3.0	1.4	3.53
1659	2.36	0.21	228.4	226.5	1.9	2.1	3.54
1759	2.33	0.21	267.1	282.1	-15.0	2.6	3.03
1859	2.93	0.14	268.4	282.5	-14.1	2.4	3.11
1933	2.74	0.15	263.3	268.5	-5.2	3.7	3.20
1938	2.80	0.15	261.0	270.2	-9.1	2.6	3.19
1944	2.83	0.14	272.2	270.4	1.7	4.8	3.19
1949	2.83	0.14	268.0	272.4	-4.4	2.1	3.18
1954	2.68	0.16	432.9	432.3	0.6	23.6	2.29
1959	2.81	0.15	250.4	250.7	-0.3	0.9	3.36
20 4	3.38	0.10	272.7	261.9	10.9	12.6	3.31
20 9	2.97	0.13	257.7	264.0	-6.2	1.1	3.26
2059	2.90	0.14	264.9	264.6	0.3	1.8	3.25
2159	3.42	0.10	248.8	250.4	-1.6	3.4	3.42
2259	3.78	0.09	234.8	245.0	-10.2	0.5	3.49
2359	3.26	0.11	225.8	236.3	-10.5	2.4	3.55
059	5.00	0.05	254.3	261.2	-6.9	1.1	3.37
159	7.50	0.03	228.2	249.0	-20.7	0.6	3.52
259	9.88	0.02	236.7	253.3	-16.6	1.7	3.49

Table 5 (Continued)

359	6.58	0.04	302.5	329.4	-26.9	2.6	2.90
459	7.60	0.03	301.1	315.3	-14.1	7.4	2.99
559	7.85	0.03	391.6	334.1	57.5	-0.9	2.88
659	8.10	0.02	289.5	306.8	-17.3	2.1	3.05
759	7.60	0.03	329.7	347.5	-17.8	3.2	2.80
859	7.85	0.03	315.4	335.0	-19.6	3.8	2.87
959	8.61	0.02	317.8	337.1	-19.4	2.6	2.86
1059	8.36	0.02	305.7	321.8	-16.1	1.1	2.96
1159	4.37	0.07	294.4	300.0	-5.6	1.3	3.05
1259	2.83	0.14	249.2	253.9	-4.7	5.1	3.34
1359	2.33	0.21	218.9	183.7	35.3	12.5	-4.07
1459	2.32	0.22	208.2	206.4	1.8	1.7	3.76
1559	2.50	0.18	232.2	233.7	-1.5	0.6	3.49
1659	2.69	0.16	242.8	251.1	-8.3	2.2	3.35
17 5	2.27	0.23	245.5	247.0	-1.5	2.8	3.31
1759	2.55	0.18	242.5	247.8	-5.3	2.4	3.36
1859	2.59	0.17	242.0	248.1	-6.1	1.3	3.36
1959	2.82	0.15	262.3	265.3	-3.0	0.4	3.24
2059	2.79	0.15	245.3	251.8	-6.5	0.5	3.35
2159	2.74	0.15	236.7	241.5	-4.8	1.6	3.44
2259	3.32	0.11	237.8	243.7	-5.9	0.7	3.47
2359	4.00	0.08	222.3	231.1	-8.8	0.8	3.64
059	4.17	0.07	217.0	231.3	-14.3	1.1	3.64
138	4.62	0.06	234.0	252.5	-18.6	5.1	3.44
146	4.71	0.06	237.9	262.4	-24.6	3.4	3.36
153	5.17	0.05	231.2	259.4	-28.2	0.5	3.39
155	4.83	0.06	225.8	213.1	12.8	27.3	-3.87
159	5.33	0.05	218.1	241.8	-23.7	1.3	3.56
2 3	6.00	0.04	219.8	246.8	-27.0	1.2	3.52
2 6	6.00	0.04	445.4	478.4	-33.0	20.2	2.24
2 9	6.20	0.04	477.3	472.4	4.8	34.0	-2.26
212	7.25	0.03	215.6	244.1	-28.5	1.3	3.56
259	7.34	0.03	248.1	274.4	-26.3	0.4	3.29
359	6.33	0.04	266.4	291.1	-24.7	0.9	3.15
459	7.09	0.03	317.2	331.9	-14.7	1.3	2.89
559	7.85	0.03	306.0	327.4	-21.4	1.6	2.92
659	8.10	0.02	311.1	326.1	-15.0	2.1	2.93
759	10.64	0.01	260.9	232.7	28.2	41.4	-3.70
8 4	8.10	0.02	236.2	232.0	4.3	0.0	3.69
8 9	8.86	0.02	234.1	207.7	26.4	14.0	-3.98
814	8.36	0.02	294.5	317.5	-22.0	1.6	2.98
819	10.38	0.02	249.4	197.0	52.3	26.2	-4.13
829	8.36	0.02	347.5	332.4	15.1	1.8	2.89
834	8.36	0.02	309.7	328.6	-18.9	1.2	2.91
839	7.09	0.03	537.6	262.3	275.3	95.4	-3.39
844	7.09	0.03	274.1	250.5	23.5	16.9	-3.50
849	8.61	0.02	290.0	304.8	-14.8	3.1	3.07
854	8.86	0.02	215.7	202.4	13.3	1.7	4.05
859	7.60	0.03	237.7	178.4	59.3	999.0	-4.40
9 9	14.69	0.01	267.2	203.4	63.8	39.3	-4.06
914	8.86	0.02	273.1	282.8	-9.7	1.6	3.23

Table 5 (Continued)

919	9.12	0.02	260.3	251.6	8.7	4.6	3.50
924	9.12	0.02	695.8	278.9	417.0	999.0	3.26
929	8.86	0.02	259.4	264.0	-4.6	1.0	3.39
934	8.86	0.02	248.7	261.7	-13.0	0.9	3.41
939	8.86	0.02	349.5	339.2	10.3	-0.2	2.85
944	9.12	0.02	270.3	284.1	-13.9	0.4	3.22
949	8.36	0.02	242.6	251.4	-8.8	1.8	3.50
954	8.86	0.02	252.3	266.2	-13.9	2.5	3.37
959	8.36	0.02	262.0	246.6	15.4	22.6	-3.54
10 4	8.61	0.02	249.8	268.4	-18.6	3.4	3.35
10 9	8.10	0.02	258.9	245.4	13.5	21.8	-3.55
1014	8.36	0.02	268.4	290.8	-22.4	2.5	3.17
1019	8.10	0.02	515.7	270.7	245.0	39.5	3.33
1024	7.85	0.03	230.8	255.0	-18.2	1.2	3.46
1029	7.60	0.03	261.4	279.7	-18.3	1.6	3.25
1034	7.60	0.03	273.8	294.6	-20.8	1.0	3.14
1039	7.34	0.03	260.4	279.1	-18.7	1.1	3.25
1044	6.58	0.04	246.0	253.3	-7.3	0.9	3.47
1049	7.34	0.03	265.4	282.9	-17.5	0.4	3.22
1054	7.34	0.03	275.5	296.3	-20.8	2.5	3.12
1059	6.84	0.03	264.1	270.9	-6.8	2.4	-3.31
11 4	7.34	0.03	275.7	294.4	-18.7	1.5	3.13
11 9	7.34	0.03	279.3	302.9	-23.6	2.0	3.08
1114	7.34	0.03	275.8	297.5	-21.7	0.7	3.11
1119	7.09	0.03	264.8	282.0	-17.3	1.3	3.23
1124	7.09	0.03	281.1	303.7	-22.6	0.5	3.07
1129	7.00	0.03	287.6	309.9	-22.3	4.6	3.02
1134	5.60	0.05	522.6	312.1	210.5	20.4	2.99
1139	5.80	0.04	302.4	319.2	-16.8	3.8	2.95
1144	4.67	0.06	310.0	308.1	1.9	1.6	3.01
1149	4.00	0.08	303.7	316.0	-12.3	1.6	2.93
1154	3.25	0.11	268.9	275.3	-6.4	2.7	3.19
1159	3.25	0.11	272.8	273.0	-0.2	2.8	-3.21
12 4	3.22	0.11	299.3	303.9	-4.6	4.3	2.98
12 9	3.33	0.11	323.4	333.1	-9.7	3.1	2.80
1214	3.22	0.11	298.6	302.9	-4.3	0.7	2.98
1219	2.90	0.14	286.2	283.0	3.2	2.0	3.10
1224	2.90	0.14	287.7	293.1	-5.4	1.4	3.03
1229	3.00	0.13	300.7	305.2	-4.5	1.1	2.95
1234	2.64	0.17	281.4	277.1	4.2	1.4	3.12
1239	2.73	0.16	299.4	299.8	-0.4	2.2	2.96
1244	2.64	0.17	294.2	275.0	19.2	16.6	-3.13
1249	2.50	0.18	283.7	276.8	6.9	1.5	3.10
1254	2.58	0.17	303.0	295.0	8.0	4.8	2.98
1259	2.58	0.17	286.3	285.5	0.8	2.0	3.05
13 4	2.31	0.22	280.9	244.8	36.1	22.4	-3.34
13 9	2.54	0.18	263.7	260.2	3.4	1.1	3.24
1314	2.54	0.18	263.4	264.6	-1.1	1.5	3.21
1319	1.89	0.36	231.2	237.6	-6.4	3.8	3.25
1329	2.71	0.16	255.1	259.2	-4.1	1.1	3.28
1334	2.29	0.22	224.3	230.2	-5.8	3.1	3.48

Table 5 (Continued)

1339	2.39	0.20	228.9	242.3	-13.4	1.2	3.38
1344	2.53	0.18	219.0	229.0	-10.0	1.0	3.54
1349	2.87	0.14	232.0	233.7	-1.7	1.8	3.54
1354	3.27	0.11	219.6	227.4	-7.8	1.6	3.64
14 4	3.71	0.09	218.6	225.9	-7.3	1.6	3.68
14 9	3.06	0.13	223.5	221.7	1.8	1.9	3.69
1414	2.94	0.13	226.4	224.4	1.9	1.4	3.65
1419	2.94	0.13	220.2	223.4	-3.2	1.5	3.66
1424	3.00	0.13	224.9	228.9	-4.0	1.6	3.60
1429	2.79	0.15	224.3	226.5	-2.2	2.0	3.61
1434	2.84	0.14	229.3	223.0	6.3	4.1	3.65
1439	2.80	0.15	226.0	219.8	6.2	1.9	3.68
1444	2.85	0.14	235.1	234.2	0.9	3.8	3.53
1449	2.55	0.18	225.3	231.7	-6.5	1.9	3.52
1454	2.57	0.18	232.7	203.5	29.2	11.1	-3.85
1459	2.24	0.24	214.5	170.4	44.1	27.9	-4.36
15 4	2.77	0.15	244.7	212.1	32.6	0.2	3.77
15 9	2.73	0.16	220.2	224.7	-4.5	1.9	3.62
1514	2.82	0.15	233.5	224.7	8.7	1.2	3.63
1519	3.14	0.12	248.7	239.8	8.9	7.2	3.50
1524	2.82	0.15	212.3	219.1	-6.8	1.2	3.69
1529	2.29	0.22	211.2	186.4	24.8	20.7	-4.02
1534	2.52	0.18	232.0	215.6	16.5	17.6	-3.69
1539	2.48	0.19	219.1	222.0	-2.9	4.1	3.61
1544	2.73	0.16	206.1	211.3	-5.2	1.9	3.77
1549	2.32	0.22	210.8	216.8	-6.0	1.9	3.63
1554	2.36	0.21	391.4	379.0	12.3	13.8	2.46
1559	2.52	0.18	222.3	225.4	-3.2	0.7	3.58
16 4	2.29	0.22	222.0	225.8	-3.8	0.6	3.53
16 9	2.29	0.22	237.4	240.0	-2.6	0.9	3.38
1614	2.33	0.21	221.2	225.9	-4.7	1.3	3.54
1619	2.58	0.17	235.5	238.9	-3.5	2.4	3.45
1624	2.44	0.19	217.6	222.9	-5.3	1.4	3.59
1629	2.44	0.19	220.3	228.2	-7.9	1.8	3.54
1634	2.44	0.19	217.8	225.5	-7.7	1.0	3.56
1639	2.52	0.18	220.7	224.3	-3.6	1.5	3.59
1644	2.48	0.19	214.9	223.7	-8.8	2.6	3.59
1649	2.52	0.18	228.3	240.7	-12.4	0.5	3.42
1654	2.59	0.17	240.0	241.8	-1.8	2.8	3.42
1659	2.46	0.19	224.1	229.4	-5.3	1.3	3.53
17 4	2.52	0.18	221.4	224.4	-2.9	0.8	3.59
17 9	2.63	0.17	226.2	230.6	-4.3	1.4	3.54
1714	2.67	0.16	234.0	237.9	-3.9	0.5	3.47
1719	2.46	0.19	234.2	207.6	26.6	23.4	-3.78
1724	2.40	0.20	220.0	222.6	-2.6	1.4	3.59
1729	2.37	0.21	218.5	224.2	-5.7	1.2	3.56
1734	2.38	0.21	214.2	217.5	-3.3	1.3	3.64
1739	2.31	0.22	221.1	224.3	-3.2	1.3	3.55
1744	2.23	0.24	221.7	231.0	-9.2	0.5	3.46
1749	2.31	0.22	227.0	231.1	-4.1	0.6	3.48
1754	2.31	0.22	220.9	225.8	-4.9	2.6	3.53

Table 5 (Continued)

1759	2.16	0.26	227.3	235.8	-8.5	4.5	3.39
18 4	2.28	0.23	240.3	243.3	-3.1	2.6	3.34
18 9	2.28	0.23	229.9	237.2	-7.3	0.7	3.40
1814	2.23	0.24	233.9	241.9	-8.0	1.5	3.35
1819	2.16	0.26	234.9	239.7	-4.8	1.5	3.35
1824	2.23	0.24	233.6	241.2	-7.7	0.3	3.35
1829	2.19	0.25	247.0	250.6	-3.6	1.3	3.25
1834	2.30	0.22	244.7	253.4	-8.7	1.6	3.26
1839	2.23	0.24	235.4	240.1	-4.7	2.6	3.36
1844	2.19	0.25	242.9	241.1	1.8	0.5	3.34
1849	2.23	0.24	238.9	244.4	-5.5	5.6	3.32
1854	2.09	0.28	243.5	241.7	1.7	2.2	3.30
1859	2.23	0.24	256.3	265.1	-8.8	1.3	3.14
19 4	2.26	0.23	241.0	244.7	-3.7	1.9	3.33
19 9	2.25	0.23	247.4	252.9	-5.5	3.8	3.25
1914	2.31	0.22	258.4	262.8	-4.5	2.9	3.18
1919	2.39	0.20	248.6	261.3	-12.7	2.5	3.21
1924	2.48	0.19	272.4	269.5	2.9	6.8	3.16
1929	2.42	0.20	254.5	256.2	-1.7	2.3	3.26
1934	2.52	0.18	264.9	269.5	-4.6	7.5	3.16
1939	2.33	0.21	253.2	256.0	-2.8	0.7	3.24
1944	2.55	0.18	264.4	269.7	-5.3	1.2	3.16
1949	2.58	0.17	258.5	262.2	-3.8	0.8	3.23
1954	2.65	0.16	267.8	269.4	-1.6	0.8	3.18
1959	2.68	0.16	257.8	263.1	-5.3	0.5	3.24

Table 5 (Continued)

ERIE MAR & APR 1985 Universal Time

TIME	X	dM	POL	DUD	DIFF	STER	M
16 4	1.54	0.76	179.7	155.2	24.4	1.8	3.85
16 9	1.54	0.76	181.3	159.8	21.5	4.0	3.77
1614	1.50	0.88	166.5	145.5	21.0	9.5	-3.88
1619	1.50	0.88	159.7	134.0	25.8	2.7	4.11
1624	1.62	0.61	210.3	178.2	32.0	4.2	3.67
1629	1.33	2.13	140.8	63.9	76.9	8.8	4.42
1634	1.58	0.67	192.0	165.7	26.2	7.4	3.78
1639	1.58	0.67	178.8	158.3	20.6	3.8	3.90
1644	1.52	0.82	180.0	151.9	28.1	0.5	3.84
1649	1.56	0.72	183.3	209.9	-26.5	3.2	3.14
1654	1.71	0.50	198.2	249.8	-51.6	36.1	2.98
1659	1.62	0.62	181.1	162.8	18.3	20.1	-3.89
17 4	1.62	0.62	298.7	176.5	122.2	6.1	3.68
17 9	1.68	0.53	170.6	180.1	-9.5	8.2	-3.73
1714	1.73	0.48	245.6	312.0	-66.4	7.9	2.55
1719	1.65	0.56	246.2	252.0	-5.7	63.8	2.90
1724	1.54	0.77	177.6	206.9	-29.3	3.4	3.12
1729	1.48	0.94	198.7	191.1	7.6	8.6	3.12
1734	1.50	0.88	177.2	190.2	-13.0	5.8	3.19
1739	1.59	0.66	260.1	214.5	45.6	2.0	3.16
1744	1.56	0.73	168.7	150.2	18.5	2.6	3.98
1749	1.44	1.09	171.6	126.1	45.5	7.7	4.00
1754	1.27	4.88	231.7	9.2	222.5	19.6	-3.16
1759	1.85	0.39	298.1	380.5	-82.4	22.9	-2.29
18 4	1.36	1.77	168.4	156.3	12.1	2.6	2.68
18 9	1.57	0.70	245.6	297.6	-52.0	7.0	2.43
1814	1.67	0.55	252.3	303.9	-51.7	6.7	2.54
1819	1.57	0.70	227.0	265.3	-38.2	10.5	-2.65
1824	1.57	0.70	320.4	266.1	54.3	20.7	-2.65
1829	1.56	0.73	234.9	256.6	-21.7	13.5	-2.69
1834	1.47	0.99	346.7	232.1	114.6	19.5	2.63
1839	1.61	0.63	265.0	292.6	-27.6	16.8	2.53
1844	1.64	0.58	272.1	279.9	-7.7	23.6	2.67
1849	1.75	0.46	265.0	299.2	-34.1	14.1	2.65
1859	1.53	0.79	274.9	237.5	37.4	2.9	2.79
19 4	1.75	0.46	254.0	257.8	-3.8	10.2	2.96
19 9	1.72	0.48	257.3	246.6	10.7	7.5	3.03
1914	1.71	0.50	267.5	246.4	21.1	1.9	3.02
1919	1.83	0.40	253.8	241.2	12.6	3.2	3.17
1924	1.81	0.42	263.2	248.6	14.6	1.3	3.09
1929	2.04	0.30	275.4	261.8	13.6	2.6	3.10
1934	1.93	0.34	251.0	239.6	11.4	2.2	3.25
1939	2.00	0.31	279.2	267.2	12.0	9.0	3.04
1944	1.93	0.34	262.0	256.0	6.1	0.6	3.10
1949	1.97	0.33	281.3	274.0	7.3	3.7	2.97
1954	1.93	0.34	263.0	248.5	14.4	1.7	3.17
1959	2.04	0.30	253.5	249.2	4.3	0.6	3.21

Table 6. Results for Erie ionograms, showing for each of the ionograms analyzed the values of X = foF2/foE; dM, the correction applied in the Dudeney model to the scaled value of M(3000)F2; the POLAN value of hmF2; the Dudeney value of hmF2; the difference (POLAN - Dudeney) between the two values of hmF2; the standard error in the POLAN value of hmF2; and the value of M(3000)F2. A negative value of M(3000)F2 indicates some uncertainty in the value.

20 4	1.90	0.36	241.3	228.0	13.3	1.0	3.35
20 9	2.00	0.31	248.3	240.6	7.6	0.9	3.28
2014	1.96	0.33	243.0	236.3	6.7	0.6	3.30
2019	1.96	0.33	245.5	240.6	5.0	1.0	3.26
2024	1.93	0.34	245.3	238.5	6.8	0.4	3.26
2029	1.93	0.34	248.8	242.1	6.6	0.5	3.23
2034	1.93	0.34	244.8	240.2	4.6	1.4	3.24
2039	1.93	0.34	247.5	239.1	8.5	0.8	3.26
2044	2.29	0.22	448.9	435.6	13.2	32.4	-2.21
2049	1.93	0.34	252.4	245.7	6.7	7.4	3.19
2054	1.96	0.33	235.8	234.7	1.1	1.2	3.32
2059	1.86	0.38	226.5	216.1	10.5	1.7	3.45
21 9	1.82	0.41	226.8	215.2	11.6	2.4	3.43
2114	1.86	0.38	242.5	230.2	12.3	4.0	3.30
2119	1.89	0.36	252.3	252.4	-0.1	5.9	3.11
2124	1.69	0.52	229.2	209.0	20.3	3.9	3.37
2129	1.81	0.41	228.2	215.0	13.2	1.9	3.43
2134	1.81	0.41	226.4	217.5	8.9	2.9	3.40
2139	1.81	0.41	241.6	229.4	12.2	6.7	3.28
2144	1.88	0.37	222.3	226.0	-3.7	4.1	3.36
2149	1.77	0.44	231.1	225.2	5.9	8.0	3.28
2154	1.77	0.44	230.5	221.9	8.6	5.6	3.32
2159	1.77	0.44	228.4	221.9	6.5	6.7	3.32
22 9	2.00	0.31	257.4	251.2	6.2	7.4	3.18
2214	1.96	0.33	236.5	234.3	2.3	3.5	3.32
2219	1.96	0.33	222.8	222.6	0.2	3.3	3.44
2224	1.88	0.37	223.7	221.8	1.9	0.6	3.40
2229	1.88	0.37	224.5	220.1	4.4	1.2	3.42
2239	1.87	0.37	208.5	206.9	1.6	2.3	3.57
2244	1.87	0.37	215.5	214.1	1.3	0.6	3.48
2249	1.83	0.40	226.6	216.9	9.6	1.9	3.42
2254	1.91	0.35	233.0	235.3	-2.3	2.9	3.28
2259	1.91	0.35	251.7	249.8	1.9	15.0	3.15
23 9	2.00	0.31	221.8	224.3	-2.5	0.6	3.44
2339	2.32	0.22	287.9	286.5	1.3	2.1	2.99
2359	2.20	0.24	271.8	273.7	-1.9	4.3	3.06
1724	1.59	0.66	201.8	189.1	12.7	12.8	3.46
1729	1.65	0.58	222.5	213.2	9.3	3.8	3.26
1734	1.65	0.58	207.9	220.4	-12.5	9.8	3.18
1739	1.61	0.62	223.9	211.3	12.7	3.7	3.23
1744	1.58	0.68	199.9	202.3	-2.4	19.1	-3.27
1749	1.65	0.58	244.2	245.7	-1.5	13.4	2.94
1754	1.53	0.79	217.4	204.9	12.5	31.5	3.12
1759	1.47	0.99	181.6	177.7	3.8	8.6	-3.23
18 4	1.65	0.58	235.7	223.0	12.7	17.7	3.16
18 9	1.59	0.66	238.3	229.9	8.4	4.2	3.00
1814	1.65	0.58	211.1	224.4	-13.4	4.5	3.14
1819	1.65	0.58	231.1	244.5	-13.4	16.1	2.95
1824	1.73	0.48	253.1	264.2	-11.1	14.3	2.89
1829	1.46	1.03	241.0	197.2	44.7	17.4	2.94

Table 6 (Continued)

1839	1.62	0.61	268.4	261.7	6.7	21.4	2.78
1844	1.62	0.61	237.3	257.0	-19.6	8.4	2.81
1849	1.62	0.61	252.7	245.0	7.7	2.1	2.91
1854	1.63	0.59	194.8	175.9	18.9	7.7	3.72
1859	1.79	0.43	241.7	253.7	-12.1	4.4	3.03
19 4	1.79	0.43	237.2	249.3	-12.1	2.8	3.07
19 9	1.79	0.43	252.5	256.6	-4.1	5.8	3.01
1914	1.79	0.43	233.4	255.4	-22.1	12.7	3.02
1919	1.66	0.56	245.1	231.2	14.0	5.5	3.09
1924	1.56	0.72	260.2	209.9	50.4	2.0	3.13
1929	1.66	0.56	229.3	223.7	5.6	6.4	3.16
1934	1.71	0.50	247.2	237.6	9.6	4.3	3.10
1939	1.55	0.75	223.2	206.4	16.7	10.3	3.14
1944	1.91	0.35	307.0	340.5	-33.5	21.8	2.51
1949	1.44	1.11	221.3	182.9	38.4	20.0	-3.03
1954	1.68	0.54	257.9	259.0	-1.1	12.1	2.87
1959	2.03	0.30	344.3	373.4	-29.0	20.4	2.40
20 4	1.65	0.58	226.0	219.5	6.5	12.5	-3.19
20 9	1.68	0.54	242.0	240.5	1.4	6.7	3.03
2014	1.62	0.61	257.7	241.7	16.0	7.3	2.94
2019	1.70	0.51	261.8	259.2	2.6	7.1	2.89
2024	1.58	0.69	250.0	228.6	21.3	1.3	2.98
2029	1.73	0.48	248.2	247.5	0.7	3.9	3.03
2034	1.68	0.54	247.9	240.5	7.4	4.7	3.03
2039	1.73	0.48	254.6	255.8	-1.2	4.7	2.96
2044	1.68	0.54	256.0	250.6	5.3	4.1	2.94
2049	1.79	0.43	244.8	259.3	-14.5	10.2	2.98
2054	1.66	0.56	263.3	245.3	18.0	1.8	2.96
2059	1.83	0.40	258.3	263.7	-5.4	9.1	2.97
21 4	1.65	0.58	231.3	227.8	3.6	12.4	-3.11
21 9	1.77	0.45	246.2	239.3	7.0	1.5	3.14
2114	1.77	0.45	250.2	243.7	6.5	2.2	3.10
2119	1.83	0.40	243.2	241.8	1.4	3.0	3.16
2124	1.77	0.45	239.3	239.3	0.0	4.0	3.14
2129	1.83	0.40	243.6	247.5	-4.0	2.8	3.11
2134	1.68	0.54	238.7	232.8	6.0	8.0	3.10
2139	1.68	0.54	237.6	233.7	3.9	3.2	3.09
2144	1.68	0.54	246.2	236.6	9.7	9.1	3.07
2149	1.68	0.54	249.8	234.1	15.7	4.8	3.09
2154	2.04	0.30	262.0	271.5	-9.5	4.0	3.02
2159	1.79	0.43	243.4	240.3	3.1	5.6	3.15
22 4	1.79	0.43	255.2	251.6	3.7	4.0	3.05
22 9	1.81	0.41	228.8	233.6	-4.8	2.9	3.23
2214	1.79	0.43	245.0	239.4	5.6	3.3	3.16
2219	1.76	0.45	239.2	237.3	2.0	2.8	3.15
2224	2.04	0.30	261.9	274.7	-12.8	5.3	3.00
2229	1.89	0.36	241.4	246.1	-4.7	3.7	3.17
2234	1.69	0.52	225.4	213.1	12.4	11.9	-3.33
2239	1.89	0.36	242.6	248.8	-6.2	4.7	3.14
2244	2.04	0.30	276.2	279.2	-3.0	9.1	2.96
2249	2.17	0.25	242.5	250.0	-7.5	0.5	3.25

Table 6 (Continued)

2254	2.16	0.26	258.0	256.1	1.9	5.0	3.19
2259	2.00	0.31	247.6	244.2	3.3	5.9	3.24
23 4	2.08	0.28	236.9	241.3	-4.4	2.5	3.31
23 9	2.04	0.29	240.3	241.9	-1.6	8.3	3.28
2314	2.22	0.24	237.8	247.1	-9.3	0.6	3.29
2319	2.00	0.31	249.3	250.1	-0.8	1.0	3.19
2324	2.12	0.27	234.9	238.3	-3.4	0.5	3.35
2329	1.88	0.37	241.2	201.5	39.7	23.0	-3.64
2334	2.17	0.25	246.0	252.1	-6.1	3.3	3.23
2339	2.23	0.24	235.4	233.5	1.9	0.9	3.43
2349	2.23	0.24	239.0	244.7	-5.6	1.5	3.32
2354	2.23	0.24	238.6	236.5	2.1	0.6	3.40
2359	2.23	0.24	247.3	247.9	-0.6	1.3	3.29
0 4	2.23	0.24	240.9	238.8	2.1	1.1	3.38
0 9	2.09	0.28	235.9	233.0	2.8	1.5	3.39
019	2.23	0.24	255.6	265.5	-9.9	4.5	3.13
049	2.47	0.19	248.0	250.0	-2.0	1.5	3.32
054	2.82	0.15	255.2	257.3	-2.1	3.7	3.31
059	2.61	0.17	248.5	244.7	3.8	1.5	3.40
1 4	2.76	0.15	245.6	245.4	0.1	1.4	3.41
1 9	2.94	0.13	264.1	266.5	-2.5	1.1	3.24
114	2.87	0.14	266.0	266.4	-0.3	2.2	3.23
119	3.07	0.12	256.7	257.9	-1.2	1.3	3.32
124	3.36	0.11	263.3	271.9	-8.5	2.7	3.22
129	3.36	0.11	261.8	267.7	-5.9	1.1	3.26
134	3.69	0.09	249.4	252.8	-3.4	1.2	3.41
139	4.00	0.08	246.1	254.6	-8.5	2.8	3.40
144	3.92	0.08	233.7	241.2	-7.5	0.8	3.53
149	4.27	0.07	241.5	250.8	-9.3	1.2	3.45
154	4.70	0.06	246.3	260.8	-14.5	1.4	3.37
159	4.70	0.06	240.2	254.0	-13.8	2.0	3.43
2 4	5.22	0.05	249.7	256.1	-6.4	1.2	3.42
2 9	5.75	0.04	245.3	262.8	-17.5	0.7	3.37
214	6.57	0.04	253.9	269.8	-15.8	2.2	3.32

Table 6 (Continued)

RICHFIELD SEP 1984 Universal Time

TIME	X	dh'	PYM	CYM	CPYM	DIFF	DIFFCP
1659	2.43	96.3	81.8	89.3	66.3	-7.5	15.4
1759	2.47	84.6	77.0	67.8	63.8	9.2	13.2
1859	2.32	115.4	100.7	96.8	85.8	3.9	14.9
1959	2.93	73.6	90.4	85.9	78.7	4.5	11.7
20 9	2.68	78.9	73.1	75.9	67.4	-2.8	5.7
2019	3.04	69.7	94.1	81.9	79.4	12.2	14.7
2029	3.07	76.0	111.0	101.7	91.8	9.4	19.2
2039	2.93	73.3	82.0	79.3	58.2	2.7	23.8
2044	3.16	64.7	75.6	64.4	45.3	11.2	30.3
2049	2.82	76.6	92.0	85.0	69.3	7.0	22.7
2054	3.08	67.4	84.0	82.6	60.0	1.5	24.0
2059	3.08	68.9	119.6	87.8	62.6	31.8	56.9
21 4	2.66	84.8	89.9	95.7	78.2	-5.8	11.7
21 9	2.66	86.0	86.6	96.9	79.0	-10.3	7.5
2114	2.66	85.4	103.2	90.1	76.7	13.2	26.6
2119	2.79	81.4	89.7	89.3	75.9	0.4	13.8
2124	2.71	80.3	85.0	78.6	79.7	6.4	5.3
2129	2.79	79.1	77.6	84.5	65.9	-6.9	11.7
2134	2.79	75.2	102.6	77.2	66.6	25.3	36.0
2139	2.89	73.0	121.4	114.9	99.5	6.5	21.9
2144	2.89	75.7	129.9	126.2	101.1	3.6	28.7
2149	2.85	73.2	112.0	107.4	93.0	4.6	19.0
2154	2.85	73.2	124.7	112.4	107.7	12.3	17.0
2159	2.81	74.1	70.6	71.5	61.9	-0.9	8.7
22 4	3.04	68.1	76.7	74.2	58.4	2.5	18.3
22 9	3.04	67.1	119.2	108.3	93.8	10.9	25.4
2214	2.74	72.0	113.3	103.4	96.2	9.9	17.1
2219	3.04	65.2	119.0	101.7	95.9	17.3	23.1
2224	3.17	60.9	98.5	66.2	54.0	32.3	44.5
2229	3.12	60.2	76.9	58.2	67.4	18.7	9.5
2234	3.30	58.4	121.3	97.2	83.4	24.1	38.0
2239	3.12	60.6	111.0	97.2	83.3	13.7	27.7
2244	3.00	62.6	77.0	72.3	69.3	4.7	7.8
2249	2.96	62.3	105.1	83.4	71.8	21.6	33.2
2254	2.96	63.3	105.1	84.0	68.6	21.1	36.5
2259	2.76	72.3	124.8	98.7	84.5	26.1	40.3
23 4	3.55	58.2	107.2	110.9	94.0	-3.6	13.3
23 9	2.83	71.3	105.4	101.9	83.4	3.5	22.0
2314	2.00	70.4	89.3	25.4	94.5	64.0	-5.1
2319	3.29	62.8	106.9	112.3	88.8	-5.3	18.2
2324	2.96	68.7	113.2	106.7	91.3	6.6	21.9
2329	4.25	41.2	110.0	75.4	71.4	34.6	38.6
2334	4.17	51.2	134.5	114.2	120.1	20.4	14.4
2339	5.00	32.6	91.8	63.6	44.7	28.2	47.1
2344	3.94	44.4	64.5	72.6	72.3	-8.1	-7.8
2349	4.37	37.1	79.9	58.2	75.6	21.7	4.3
2354	4.25	37.5	50.6	60.1	44.5	-9.4	6.1

Table 7. Results for Richfield ionograms for the parabolic half-width ymF2. The parameter X is defined as X = foF2/foE; dh' is the difference between the virtual height and calculated real height at fmin; PYM is the value of ymF2 deduced using the POLAN N(h) profile; CYM is the value of ymF2 obtained using the CCIR formula and the Dudeney value of hmF2; CPYM is the value of ymF2 obtained using the CCIR formula, and the POLAN value of hmF2; DIFF is the difference PYM - CYM; and DIFFCP is the difference PYM - CPYM.

2359	2.44	42.5	25.8	-5.3	71.2	31.1	-45.4
014	2.87	41.7	14.6	22.6	33.7	-8.1	-19.2
019	4.21	35.2	64.6	57.6	67.2	7.0	-2.6
024	4.29	41.4	82.4	93.0	78.4	-10.7	4.0
029	4.07	42.7	76.7	61.5	72.7	15.2	4.0
034	4.92	44.9	126.9	134.6	120.5	-7.7	6.3
039	4.31	40.0	67.3	77.1	62.4	-9.8	4.9
044	4.31	43.9	74.6	98.9	78.9	-24.3	-4.3
049	4.50	40.0	89.5	85.9	76.6	3.7	13.0
059	4.58	43.0	87.1	107.8	80.0	-20.7	7.1
1 4	5.00	40.5	103.5	113.2	87.4	-9.7	16.0
114	5.60	33.3	99.8	81.6	69.7	18.1	30.0
119	6.00	31.9	97.5	81.0	66.2	16.4	31.2
124	7.00	27.6	118.0	93.2	79.6	24.8	38.4
129	6.56	24.6	91.0	64.2	55.7	26.9	35.3
134	7.50	21.8	95.7	64.5	49.3	31.3	46.5
144	8.29	19.0	90.0	61.7	45.5	28.4	44.5
154	9.83	18.3	105.2	88.0	75.5	17.2	29.7
159	9.33	18.3	110.1	79.2	71.1	30.9	39.0
2 4	10.60	14.9	79.1	65.0	46.2	14.0	32.8
2 9	9.60	13.9	74.9	47.7	34.2	27.2	40.8
859	7.60	29.3	96.4	74.7	54.6	21.6	41.8
959	7.85	32.1	88.7	76.7	60.4	12.0	28.2
1059	8.36	30.6	125.1	109.4	81.5	15.7	43.6
1159	4.25	47.3	72.0	82.2	69.3	-10.2	2.7
1259	2.92	72.1	77.6	114.3	104.7	-36.7	-27.1
1359	2.87	58.1	46.9	65.7	62.2	-18.8	-15.3
1459	2.68	74.3	100.3	94.9	81.8	5.4	18.5
1559	2.96	58.8	87.9	74.2	62.7	13.8	25.3
1659	2.36	80.7	77.2	80.5	78.2	-3.2	-0.9
1759	2.33	119.9	146.0	177.0	143.9	-31.0	2.1
1859	2.93	80.4	132.7	120.6	92.9	12.1	39.8
1933	2.74	83.3	91.7	93.1	76.0	-1.4	15.7
1938	2.80	80.9	84.0	88.9	67.6	-4.9	16.4
1944	2.83	79.5	138.1	118.0	112.4	20.0	25.7
1949	2.83	80.1	117.0	87.4	73.9	29.6	43.2
1954	2.68	170.3	191.2	72.0	62.4	119.2	128.7
1959	2.81	71.7	55.0	48.4	39.2	6.6	15.8
20 4	3.38	57.9	79.2	60.8	67.4	18.4	11.9
20 9	2.97	70.9	74.3	77.4	61.3	-3.1	13.0
2059	2.90	74.2	88.5	87.4	79.1	1.1	9.5
2159	3.42	52.8	91.1	75.8	66.8	15.3	24.3
2259	3.78	45.0	116.2	107.1	84.6	9.1	31.6
2359	3.26	50.9	63.1	64.2	43.6	-1.1	19.5
059	5.00	35.0	78.2	79.9	64.1	-1.6	14.2
159	7.50	20.9	76.5	76.9	44.9	-0.4	31.5
259	9.88	16.0	62.5	42.0	23.1	20.5	39.4
359	6.58	35.2	114.9	77.4	52.3	35.5	60.6
459	7.60	29.5	115.2	56.5	34.2	58.7	81.0
559	7.85	31.0	348.6	16.6	75.8	332.0	272.8
659	8.10	26.5	77.5	37.2	11.3	40.4	66.3

Table 7 (Continued)

759	7.60	32.7	110.6	88.4	70.7	22.3	39.9
859	7.85	30.5	103.1	70.2	45.6	33.0	57.5
959	8.61	28.5	112.1	96.5	68.2	15.5	43.9
1059	8.36	27.4	95.7	80.0	55.6	15.7	40.2
1159	4.37	51.0	85.1	89.7	75.4	-4.6	9.7
1259	2.83	72.3	72.5	117.7	106.3	-45.2	-33.8
1359	2.33	56.9	64.3	15.2	65.4	49.1	-1.1
1459	2.32	71.7	69.0	63.7	57.3	5.2	11.7
1559	2.50	77.1	58.3	55.5	45.8	2.8	12.5
1659	2.69	76.1	84.8	88.7	70.2	-3.9	14.7
17 5	2.27	102.9	112.0	115.0	103.8	-3.0	8.2
1759	2.55	81.7	69.7	66.0	51.5	3.7	18.1
1859	2.59	80.1	80.5	67.5	51.5	13.0	29.0
1959	2.82	77.1	78.2	69.3	58.5	8.9	19.7
2059	2.79	72.2	72.2	68.7	52.2	3.5	20.1
2159	2.74	69.4	123.6	100.5	86.4	23.1	37.1
2259	3.32	52.5	106.4	75.9	61.4	30.5	45.0
2359	4.00	37.4	49.6	54.0	35.7	-4.4	13.9
059	4.17	35.7	80.3	82.9	57.2	-2.6	23.0
138	4.62	36.3	86.2	89.7	58.1	-3.5	28.1
146	4.71	38.0	96.2	91.9	52.2	4.3	44.0
153	5.17	33.3	85.8	78.7	36.5	7.1	49.3
155	4.83	25.5	69.3	6.0	13.6	63.3	55.7
159	5.33	29.1	60.0	49.3	10.4	10.7	49.7
2 3	6.00	26.0	70.6	59.4	19.9	11.2	50.7
2 6	6.00	64.6	200.5	74.0	40.4	126.4	160.0
2 9	6.20	59.9	217.2	54.8	81.1	162.4	136.2
212	7.25	20.5	66.1	46.4	12.1	19.8	54.0
259	7.34	24.6	76.6	66.4	37.0	10.2	39.6
359	6.33	30.6	84.8	80.4	56.1	4.4	28.6
459	7.09	33.1	89.3	59.3	44.7	30.0	44.6
559	7.85	30.1	97.8	68.8	38.3	29.0	59.5
659	8.10	28.9	91.9	71.2	47.9	20.7	44.0
759	10.64	12.1	81.8	36.7	71.7	45.1	10.0
8 4	8.10	16.4	-10.9	-18.0	-14.5	7.1	3.6
8 9	8.86	12.6	61.0	20.2	44.1	40.8	16.9
814	8.36	27.0	99.1	51.4	17.9	47.8	81.2
819	10.38	9.1	65.3	0.5	58.7	64.8	6.6
829	8.36	27.9	55.5	93.7	112.3	-38.2	-56.8
834	8.36	27.9	101.1	78.7	54.9	22.4	46.2
839	7.09	23.4	310.6	-294.5	18.2	605.1	292.4
849	8.61	24.6	84.5	50.2	27.2	34.3	57.3
854	8.86	12.5	48.9	16.8	21.1	32.1	27.7
859	7.60	9.7	999.9	-17.0	53.3	999.9	999.9
9 9	14.69	7.1	83.4	8.4	76.2	75.0	7.1
914	8.86	21.1	66.2	38.0	22.6	28.2	43.6
919	9.12	17.7	89.5	74.2	72.9	15.3	16.7
924	9.12	20.1	999.9	88.3	547.4	999.9	999.9
929	8.86	19.0	53.3	19.7	9.9	33.6	43.4
934	8.86	18.5	56.8	27.1	10.4	26.7	43.4
939	8.86	27.7	77.4	-16.6	-9.7	93.9	87.0

Table 7 (Continued)

944	9.12	20.1	71.2	48.3	33.9	22.9	37.2
949	8.36	19.5	43.3	67.9	44.6	-24.6	-1.2
954	8.86	20.0	62.6	91.7	64.5	-29.1	-1.9
959	8.36	18.6	75.4	56.6	63.9	18.8	11.5
10 4	8.61	20.4	61.5	50.7	22.2	10.8	38.4
10 9	8.10	17.8	75.4	30.2	46.0	45.2	29.3
1014	8.36	22.7	103.2	101.9	78.6	1.3	24.7
1019	8.10	22.1	405.2	-176.7	90.4	581.9	314.8
1024	7.85	22.7	58.8	94.9	49.2	-36.1	9.6
1029	7.60	24.6	73.7	75.6	47.8	-1.9	25.9
1034	7.60	25.5	82.1	43.2	21.8	38.9	60.3
1044	6.58	23.3	48.5	30.2	23.5	18.3	25.0
1054	7.34	28.0	91.4	96.6	64.7	-5.2	26.7
1059	6.84	25.7	65.0	54.6	43.5	10.4	21.5
11 9	7.34	28.6	90.1	94.1	61.5	-4.0	28.6
1114	7.34	28.2	83.0	83.2	50.1	-0.2	33.0
1119	7.09	26.8	70.4	69.9	43.4	0.5	27.1
1124	7.09	29.0	92.1	82.3	57.1	9.8	35.0
1129	7.00	31.6	100.7	107.3	72.5	-6.6	28.3
1134	5.60	39.3	69.5	-87.8	162.0	157.4	-92.5
1139	5.80	38.7	98.8	86.6	68.7	12.2	30.0
1144	4.67	47.4	68.0	104.7	108.4	-36.7	-40.4
1149	4.00	59.6	101.9	119.7	105.5	-17.8	-3.5
1159	3.25	62.8	77.6	69.5	71.9	8.1	5.7
12 4	3.22	77.4	95.2	110.3	99.2	-15.2	-4.1
12 9	3.33	82.1	118.9	138.5	128.7	-19.6	-9.8
1214	3.22	77.9	88.9	112.4	98.6	-23.5	-9.6
1219	2.90	82.2	81.5	100.9	98.8	-19.4	-17.4
1224	2.90	85.9	91.9	112.9	101.2	-21.0	-9.3
1229	3.00	87.0	97.2	129.5	118.1	-32.4	-20.9
1249	2.50	101.3	84.5	117.0	126.2	-32.5	-41.7
1254	2.58	106.1	106.6	146.4	154.9	-39.8	-48.3
1259	2.58	99.3	92.9	127.0	131.0	-34.0	-38.1
13 4	2.31	99.9	63.4	80.6	104.0	-17.2	-40.6
13 9	2.54	89.3	69.9	93.3	102.0	-23.5	-32.1
1314	2.54	92.6	74.5	112.7	113.2	-38.2	-38.6
1319	1.89	147.6	122.7	135.4	116.4	-12.7	6.3
1334	2.29	88.2	82.5	82.3	68.1	0.2	14.4
1339	2.39	89.7	114.8	107.3	78.9	7.5	35.9
1344	2.53	73.0	82.2	84.4	63.4	-2.2	18.8
1349	2.87	60.7	59.5	69.2	67.4	-9.7	-7.9
1354	3.27	48.3	50.3	52.3	32.6	-2.0	17.7
14 4	3.71	39.7	45.5	46.4	29.2	-0.8	16.3
14 9	3.06	50.7	42.6	56.0	50.1	-13.3	-7.4
1419	2.94	54.6	49.3	61.6	47.1	-12.3	2.2
1424	3.00	55.7	48.6	78.9	62.1	-30.3	-13.5
1434	2.84	58.2	78.0	71.1	69.4	7.0	8.6
1439	2.80	57.6	41.5	56.4	56.0	-14.9	-14.4
1444	2.85	61.9	88.2	86.1	80.1	2.1	8.1
1449	2.55	73.9	94.8	93.6	75.1	1.2	19.7
1454	2.57	57.4	92.5	48.7	85.6	43.8	6.9

Table 7 (Continued)

1459	2.24	50.3	95.5	12.4	80.9	83.1	14.6
15 4	2.77	54.2	13.1	53.8	94.7	-40.7	-81.5
15 9	2.73	62.1	74.9	69.6	54.8	5.3	20.1
1514	2.82	58.8	43.4	56.5	61.4	-13.1	-18.0
1519	3.14	55.9	90.1	71.9	75.6	18.2	14.5
1524	2.82	55.4	87.2	68.2	52.7	19.0	34.5
1529	2.29	58.5	83.9	43.5	78.9	40.4	5.0
1534	2.52	66.0	69.7	56.8	74.3	12.9	-4.6
1539	2.48	71.9	70.0	69.3	56.2	0.7	13.9
1544	2.73	57.2	47.8	59.7	38.9	-11.9	8.9
1549	2.32	78.5	94.3	96.0	76.5	-1.7	17.8
1554	2.36	195.4	178.8	137.1	107.8	41.7	71.0
1559	2.52	72.3	62.6	64.2	49.2	-1.6	13.4
16 4	2.29	86.7	70.8	82.7	67.5	-12.0	3.2
16 9	2.29	97.0	106.4	118.2	103.5	-11.7	2.9
1614	2.33	83.9	60.4	66.0	48.0	-5.6	12.4
1619	2.58	75.9	77.1	72.1	59.3	5.0	17.8
1624	2.44	74.0	49.4	56.7	40.6	-7.4	8.8
1629	2.44	77.4	60.4	78.4	57.3	-18.0	3.0
1634	2.44	75.7	113.3	121.3	100.9	-7.9	12.5
1639	2.52	72.3	51.6	59.2	41.8	-7.6	9.9
1644	2.48	73.4	87.0	83.7	59.4	3.3	27.7
1649	2.52	79.7	81.9	89.5	63.7	-7.6	18.3
1654	2.59	77.5	75.8	73.1	60.6	2.6	15.2
1659	2.46	77.6	60.6	63.4	44.8	-2.8	15.7
17 4	2.52	71.3	54.9	51.2	37.9	3.7	17.0
17 9	2.63	69.9	55.9	54.9	37.8	1.1	18.2
1714	2.67	71.1	68.5	66.6	53.0	1.8	15.5
1719	2.46	64.2	67.1	27.3	60.9	39.8	6.2
1724	2.40	77.3	61.6	68.6	54.4	-6.9	7.2
1729	2.37	80.2	63.4	70.2	51.4	-6.8	12.0
1734	2.38	74.3	50.7	51.2	38.6	-0.5	12.1
1739	2.31	83.3	87.0	77.1	64.3	10.0	22.8
1744	2.23	94.2	75.5	87.2	63.6	-11.7	11.9
1749	2.31	88.5	67.1	72.5	56.7	-5.4	10.4
1754	2.31	85.2	91.6	81.8	64.0	9.8	27.5
1759	2.16	105.8	82.6	99.7	74.6	-17.1	8.0
18 4	2.28	99.2	114.7	129.7	116.6	-15.0	-1.9
18 9	2.28	95.5	77.3	80.8	59.2	-3.5	18.1
1814	2.23	102.3	101.5	89.1	66.9	12.4	34.6
1819	2.16	108.2	103.4	95.2	70.2	8.2	25.3
1824	2.23	102.3	82.1	89.1	66.4	-7.0	15.7
1829	2.19	114.5	103.3	117.3	98.5	-13.9	4.8
1834	2.30	103.5	103.4	91.0	69.5	12.4	33.9
1839	2.23	102.1	70.5	72.7	55.1	-2.2	15.3
1844	2.19	107.6	77.1	87.6	79.4	-10.6	-2.3
1849	2.23	105.2	83.8	95.1	76.3	-11.3	7.5
1854	2.09	118.1	113.4	104.4	99.3	9.0	14.1
1859	2.23	120.3	107.8	116.1	91.2	-8.3	16.6
19 4	2.26	102.7	104.2	81.0	64.5	23.2	39.8
19 9	2.25	109.7	86.8	94.2	73.5	-7.5	13.3

Table 7 (Continued)

1914	2.31	108.8	101.6	108.6	93.8	-7.0	7.8
1919	2.39	101.9	91.1	96.2	66.7	-5.0	24.5
1924	2.48	99.3	134.0	102.0	97.6	32.0	36.4
1929	2.42	95.4	82.5	80.9	71.3	1.6	11.2
1934	2.52	96.7	103.1	106.3	91.1	-3.2	12.0
1939	2.33	103.3	88.6	92.7	78.4	-4.1	10.2
1944	2.55	94.2	97.3	93.1	78.2	4.2	19.0
1949	2.58	88.4	79.0	80.6	67.1	-1.6	11.9
1954	2.65	88.4	124.3	92.9	82.8	31.5	41.6
1959	2.68	83.7	79.2	77.6	60.9	1.6	18.3

Table 7 (Continued)

2.0 SIMPLE MODELS OF THE IONOSPHERE

Simple models of the ionosphere have been used for many years in applications in which the errors in the resulting calculations are accepted because of the enormous decrease in computation times which such models permit. One of the most important practical applications is in the calculation of sky-wave field strengths and transmission losses at HF. See, for example, the Supplement to Report 252 [CCIR, 1980]. For these calculations, the propagation modes involving reflection from the E and F layers are determined using an ionospheric model with parameters which depend on the routinely scaled values of foE, foF2, M(3000)F2 and h'F,F2.

The model currently recommended by CCIR consists of:

a parabolic E layer below its height of maximum electron density, hmE, with semi-thickness ymE. hmE and ymE are set to 110 km and 20 km respectively.

a parabolic F2 layer with height of maximum density hmF2, and semi-thickness ymF2.

a linear increase of electron density between hmE and the point on the parabolic F2 layer where the plasma frequency is 1.7 foE.

The model parameters hmF2 and ymF2 are given by the empirical equations [Bradley and Dudeney, 1973; CCIR, 1980]:

$$hmF2 = 1490/[M(3000)F2 + dM] - 176$$

with $$dM = 0.18/(X - 1.4) + 0.096\ (R12 - 25)/150$$

and $$X = foF2/foE, \text{ or } 1.7,$$

whichever is the larger. R12 is the 12-month smoothed sunspot number.

$$ymF2 = hmF2 - h'F,F2 + dh'$$

where $$dh' = [0.613/(X - 1.33)]^{0.86} \cdot (hmF2 - 104).$$

ymF2 is constrained to lie between 35 km and (hmF2 - hmE).

The term dM is an empirical correction term which takes into account the effects of underlying ionization not allowed for in the original Shimazaki [1955] formulation. Model estimates of hmF2 are usually correct to within 20 to 30 km [CCIR, 1980]. Dudeney [1983] has described an improved model which uses a cosine F2 layer shape and a more realistic E-F transition region, and has deduced that this model yields more accurate values of hmF2 than the Bradley-Dudeney model. Dudeney gives a revised formula for hmF2:

$$hmF2 = 1490\ F/(M + dM) - 176$$

where $$dM = 0.253/(X - 1.215) - 0.012$$

and $$F = [(0.0196\ M^2 + 1)/(1.2967\ M^2 - 1)]^{0.5}.$$

The value of X is constrained to exceed 1.215.

In this report we have used the Dudeney formula for hmF2, and the CCIR formula for ymF2. The value of foE at night was not permitted to go below the minimum value recommended by CCIR [1980]:

$$foE = [0.017\ (1 + 0.0098\ R12)^2]^{0.25}.$$

We have re-evaluated the value of M(3000)F2 using the auto-scaled trace, in order to be exactly consistent with the URSI standards [Piggott and Rawer, 1982]. Paul [1982] has shown that the M factor table given by Piggott and Rawer can be represented to within 0.5% by the expression

$$m = (67.654 - 0.0149\ h')/h'^{0.5}.$$

The MUF(3000)F2 is obtained by finding the maximum of the product f and m, and then division by foF2 yields the value of M(3000)F2.

The height difference dh corresponding to a difference dM in the derived M value is approximately given by

$$dh = - 1490/M^2 \, dM.$$

For M = 3, dh = -165 dM. The discrepancies between the ARTIST-scaled values and the Paul value were typically 0.05, the ARTIST values being too low. The ARTIST values of hmF2 would thus be typically too high by about 8 km, which is large compared to the average errors we have found in the model values of hmF2. ULCAR has therefore decided to implement Paul's approach to determining M(3000)F2 in the ARTIST software.

3.0 DISCREPANCIES BETWEEN POLAN AND SIMPLE MODEL VALUES OF hmF2 AND ymF2

3.1 Discrepancies in hmF2

We have analyzed the differences between the POLAN and Dudeney values of hmF2 according to the value of X (= foF2/foE) and to the value of the correction term dM. The differences have been distributed among bins 5 km wide, with extreme negative values being placed in the <-30 km bin, and extreme positive values being placed in the >30 km bin. Negative discrepancies indicate that the POLAN value was less than the Dudeney value.

Table 8 shows the distributions of the discrepancies for dM values of 0.0 to 0.1, while Table 9 shows the distribution for dM from 0.11 to 0.5. Broadly speaking, the low values of dM (Table 8) correspond to nighttime ionograms, and the high values to daytime ionograms. It can be seen that the Dudeney result is systematically higher than the POLAN result at night, by about 15 ± 15 km. During the day, there is no significant systematic discrepancy between the two sets of results, and 81% of the discrepancies lie within ± 10 km. [Note that the extreme values are ignored when calculating the percentages.] There were 69 Argentia and Erie ionograms for which dM exceeded 0.5. When the discrepancies greater than 30 km are ignored, the average discrepancy for the remaining 48 cases was 15 - 20 km, the Dudeney values being the larger.

Tables 10 to 14 show the distributions of the discrepancies for four ranges of X, and for all data. The summary table, Table 14, shows that the discrepancies change from being systematically positive for low X values, to being systematically negative for large X values. The average

ΔhmF2 (km)	LOW	ARG	GB	UTAH	ERIE	TOTAL	%
< -30	2	29	3	1	0	35	-
-30 -25	3	18	7	5	0	33	11
-25 -20	4	24	4	13	0	45	15
-20 -15	11	31	9	19	2	72	23
-15 -10	9	18	1	16	2	46	15
-10 - 5	8	12	2	20	4	46	15
- 5 0	5	4	2	9	1	21	7
0 5	7	2	0	4	0	13	4
5 10	2	2	1	2	0	7	2
10 15	2	1	0	8	0	11	4
15 20	4	0	0	3	0	7	2
20 25	2	1	0	1	0	4	1
25 30	0	2	0	2	0	4	1
> 30	4	6	3	8	0	21	-
N	63	150	32	111	9	365	309

Table 8. Distribution of discrepancies between the POLAN and Dudeney values of hmf2, for $0.0 \leq dM < 0.10$ (Night). A positive value of ΔhmF2 indicates that the POLAN value was greater than the Dudeney value.

ΔhmF2 (km)	LOW	ARG	GB	UTAH	ERIE	TOTAL	%
< -30	0	1	0	0	5	6	-
-30 -25	0	0	0	0	1	1	0
-25 -20	0	0	0	0	1	1	0
-20 -15	0	1	1	0	0	2	0
-15 -10	2	3	2	9	5	21	4
-10 - 5	3	11	4	50	10	78	16
- 5 0	6	29	8	61	22	126	27
0 5	6	49	4	24	25	108	23
5 10	4	34	9	7	19	73	15
10 15	3	11	4	2	14	34	7
15 20	2	8	1	3	0	14	3
20 25	3	2	2	1	1	9	2
25 30	0	5	0	2	0	7	1
> 30	6	3	5	6	1	21	-
N	35	157	40	165	104	501	474

Table 9. Distribution of discrepancies between the POLAN and Dudeney values of hmF2, for $0.11 \leq dM \leq 0.50$ (Day)

ΔhmF2 (km)	LOW	ARG	GB	UTAH	ERIE	TOTAL	%
< -30	0	0	0	0	8	8	-
-30 -15	0	0	0	0	3	3	1
-25 -20	0	0	0	0	2	2	1
-20 -15	0	0	0	0	1	1	0
-15 -10	0	1	0	0	8	9	4
-10 - 5	0	4	0	0	5	9	4
- 5 0	1	13	0	0	14	28	11
0 5	0	28	0	0	21	49	20
5 10	2	28	4	0	31	65	26
10 15	1	16	1	0	19	37	15
15 20	0	12	1	0	7	20	8
20 25	2	7	2	0	7	18	7
25 30	0	9	0	0	3	12	5
> 30	7	8	2	0	13	30	-
N	13	126	10	0	142	291	250

Table 10. Distribution of discrepancies between the POLAN and Dudeney values of hmF2, for $0.0 \leq X \leq 2.0$.

ΔhmF2 (km)	LOW	ARG	GB	UTAH	ERIE	TOTAL	%
< -30	0	2	0	0	0	2	-
-30 -25	0	2	0	0	1	3	1
-25 -20	0	0	0	0	0	0	0
-20 -15	0	4	1	0	0	5	1
-15 -10	2	4	2	11	1	20	6
-10 - 5	8	10	4	52	10	84	24
- 5 0	6	18	8	62	12	106	31
0 5	7	26	4	24	9	70	20
5 10	3	10	5	8	0	26	8
10 15	3	2	3	3	2	13	4
15 20	2	4	0	3	0	9	3
20 25	2	1	0	1	0	4	1
25 30	0	1	0	2	0	3	1
> 30	1	0	3	5	0	9	-
N	34	84	30	171	35	354	343

Table 11. Distribution of discrepancies between the POLAN and Dudeney values of hmF2, for $2.01 \leq X \leq 4.0$.

ΔhmF2 (km)	LOW	ARG	GB	UTAH	ERIE	TOTAL	%
< -30	0	26	1	1	0	28	-
-30 -25	0	6	1	2	0	9	10
-25 -20	0	7	0	2	1	10	11
-20 -15	1	12	0	4	2	19	20
-15 -10	2	6	0	3	2	13	14
-10 - 5	0	7	1	8	0	16	17
- 5 0	1	2	2	4	0	9	10
0 5	2	0	0	2	0	4	4
5 10	0	2	1	0	0	3	3
10 15	1	1	0	4	0	6	6
15 20	1	0	0	1	0	2	2
20 25	0	1	0	0	0	1	1
25 30	0	2	0	0	0	2	2
> 30	1	5	0	1	0	7	-
N	9	77	6	32	5	129	94

Table 12. Distribution of discrepancies between the POLAN and Dudeney values of hmF2, for $4.01 \leq X \leq 6.0$.

ΔhmF2 (km)	LOW	ARG	GB	UTAH	ERIE	TOTAL	%
< -30	3	2	2	0	0	7	-
-30 -25	3	10	6	3	0	22	12
-25 -20	4	17	4	11	0	36	20
-20 -15	12	16	9	15	1	53	29
-15 -10	8	10	1	11	0	30	17
-10 - 5	3	2	1	9	0	15	8
- 5 0	2	1	0	4	0	7	4
0 5	2	0	0	2	0	4	2
5 10	1	0	0	1	0	2	1
10 15	0	0	0	3	0	3	2
15 20	2	0	0	2	0	4	2
20 25	1	0	0	1	0	2	1
25 30	0	0	0	2	0	2	1
> 30	3	1	3	7	0	14	-
N	44	59	26	71	1	201	180

Table 13. Distribution of discrepancies between the POLAN and Dudeney values of hmF2, for X > 6.0.

ΔhmF2 (km)	0-2.00	2.01-4.00	4.01-6.00	>6.0	TOTAL %
-30 -25	1	1	10	12	6
-25 -20	1	0	11	20	8
-20 -15	0	1	20	29	13
-15 -10	4	6	14	17	8
-10 - 5	4	24	17	8	13
- 5 0	11	31	10	4	14
0 5	20	20	4	2	12
5 10	26	8	3	1	9
10 15	15	4	6	2	7
15 20	8	3	2	2	4
20 25	7	1	1	1	2
25 30	5	1	2	1	3
N	250	343	94	180	

Table 14. Percentage distribution of discrepancies less than 30 km for all five stations, for four ranges of X.

discrepancy is about -5 km, but this value is partly a reflection of the numbers of cases in the different ranges of X. Generally speaking, the high X values correspond to nighttime conditions. For $X \leq 6$, the discrepancy can be expressed as

$$dhmF2 = 12.5 - 5\ X \text{ km}.$$

Note that this result may be peculiar to the data base used in the present analysis. Figure 1 represents the results of Table 14 in form of a diagram.

The least-squares fit linear relation between dhmF2 and X for absolute values of dhmF2 not greater than 30 km is

$$dhmF2 = 8.63 - 2.99\ X,$$

and the correlation coefficient is -0.55. However, this fit is heavily weighted by the data points for X less than 4.0, and is not a good fit for the data with X greater than 4.0.

We have not considered the discrepancies between the CCIR/Bradley-Dudeney and POLAN results in any detail, since the differences between the parabolic and cosine model results are in most cases smaller than the differences of either from the POLAN results.

The systematically high values of hmF2 given by the Dudeney formula at night can be traced to the model's neglect of underlying ionization. The effect of this underlying ionization was originally considered to be insignificant a decade or so ago, which it indeed was in comparison with the effect of the E and F1 layers during the day. However, the daytime models have been improved to the point where the nighttime errors are now the largest obtained.

In order to support this contention, we must first ensure that the source of the discrepancies does not lie with POLAN. We provide three sets of results that show that the

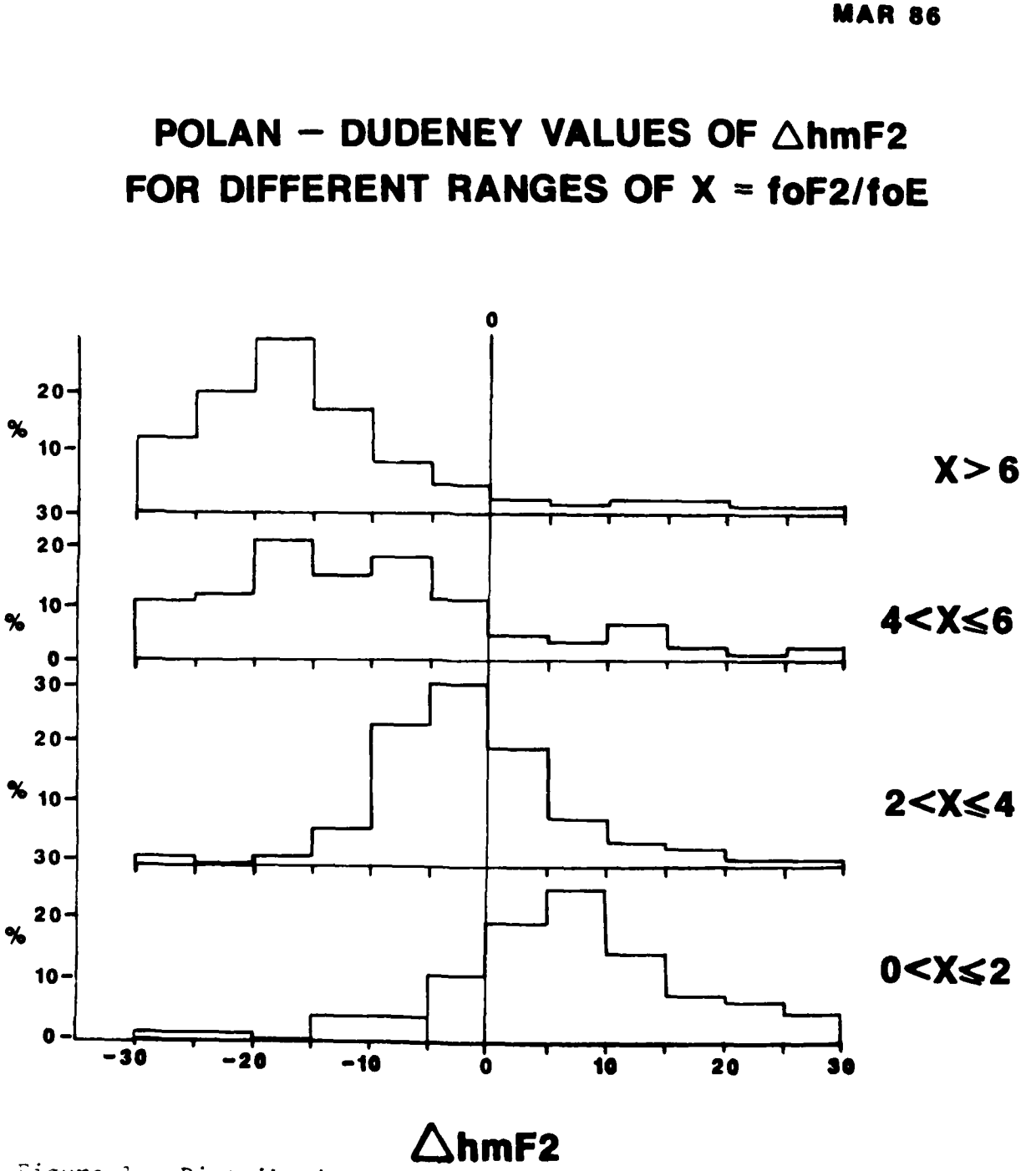

Figure 1. Distribution of the discrepancies in km between the POLAN and Dudeney values of the height of the F2-layer peak, hmF2. The ordinates are percentages, and values lying outside the 30 km limits have been ignored. The parameter S is defined by X = foF2/foE.

POLAN results are the more accurate ones. Firstly, we have analyzed the virtual heights for a parabolic layer with hmF2 = 260 km, ymF2 = 60 km and foF2 = 6 MHz, using the no-field formula for h', which we simulated for POLAN by using a dip angle of zero. There was no ionization below 200 km. The small error in the POLAN result of hmF2 = 261.3 can be attributed to our use of a "direct start" for POLAN, in which the real height at fmin, which we set to 0.5 MHz, was set equal to the virtual height. The Dudeney model gave a value of 260.2 km.

Our second test was on an ionogram calculated numerically for a profile composed of two overlapping Chapman layers. The layer parameters were 0.5 MHz, 3.0 MHz, 115 km, 300 km, 10.0 km and 60.0 km, for the E and F layer values of critical frequency, peak height and scale height. We took fmin = 1.5 MHz, and included five extraordinary ray points at the start for POLAN to use to start the analysis. The test simulated typical nighttime conditions. In this case, the POLAN result was about 10 km too low, mainly because POLAN found a real height at fmin of 172 km, instead of the correct value of 198 km. Since the error drops off only as 1/f, it had decreased by only about 1/2 by the time the peak was reached. The Dudeney model, on the other hand, gave a result which was 29 km too high. Thus even though the POLAN result was in error, the error in the Dudeney result was three times as great.

Finally, we have analyzed the same set of ionograms using three of the starting options provided by POLAN. Table 15 shows the values of hmF2 for six Argentia ionograms analyzed using a synoptic model start, a direct start in which h(1) = h'(1) and an extrapolated start. In a direct start, no allowance is made for any underlying ionization. In an extrapolated start, the first few virtual heights are

TIME (UT)	h(fmin) SYN	h(fmin) EXT	h(fmin) DIR	hmF2 SYN	hmF2 EXT	hmF2 DIR	hmF2 DUD
2209	198	183	287	274	264	326	310
2219	189	211	257	264	274	295	290
2224	187	193	265	272	277	307	307
2231	204	182	287	306	292	354	356
2237	205	211	290	281	284	317	311
2244	208	182	297	338	323	389	384

Table 15. Values of real heights deduced for fmin and foF2 (hmF2), using the synoptic, extrapolated and direct start options of POLAN, and the Dudeney model. Argentia ionograms, February 1986.

extrapolated downwards in frequency, to obtain reasonable values of h' at frequencies below fmin. The ionograms chosen yielded hmF2 discrepancies greater than 30 km. In all six cases, the Dudeney results lie closest to the direct start results, which make no allowance for underlying ionization. At fmin, the delay caused by ionization below fmin is typically 80 km. Again, Titheridge [1985, Figure A2] has shown that a 5 km error in the starting height will result in a 1 km error at a plasma frequency of twice the gyrofrequency. Thus for POLAN to yield an underestimate of about 20 km at the typical nighttime foF2 of 3 MHz, or twice the gyrofrequency, the synoptic model value for the real height at 0.5 MHz must be too low by about 100 km. This is clearly impossible.

We conclude therefore that a large part of the discrepancies between the POLAN and Dudeney results for hmF2 at night can be attributed to the neglect by the Dudeney model of the underlying ionization.

3.2 Discrepancies in ymF2

We have considered the discrepancies between the POLAN and CCIR values of the semi-thickness ymF2 only for the Richfield, Utah ionograms. The POLAN value of ymF2 was found by determining the parabola which passed through (foF2, hmF2) and the real height calculated for the frequency at which ARTIST found the value of h'F or h'F2. The scale height of the Chapman peak fitted by POLAN was not considered appropriate, since it is characteristic of the very peak of the layer, rather than of the layer as a whole. The value of hmF2 required by the CCIR formula was set to the Dudeney and POLAN values in turn, giving two sets of discrepancies. These are listed in Table 7 as CYM, the CCIR value based on

the Dudeney value of hmF2, and CPYM, the CCIR value based on the POLAN value of hmF2. The former set is probably the most self-consistent, since the formula for ymF2 is based on a simple parabolic model.

Table 16 shows the percentage distribution of discrepancies in CYM for different ranges of X. For $X \leq 6$, the median discrepancy is 5 km and approximately 2/3 of the values lie within 15 km of this value. For higher values of X, the CCIR value is systematically higher than the POLAN result by about 20 km. We have not studied the discrepancies in detail because of the large proportion of excessively high discrepancies also obtained, and because we consider that the systematic biases in the simple model values of hmF2 at night must first be removed. This can be done only with a much larger and perhaps more representative data base.

ΔymF2	0.0-3.00	3.01-6.00	0.0-6.0	>6.0
< -35	1	0	1	0
-35 -30	3	2	3	3
-30 -25	3	0	2	0
-25 -20	1	2	1	2
-20 -15	1	5	3	2
-15 -10	3	5	4	0
-10 - 5	10	5	8	0
- 5 0	13	10	12	3
0 5	13	15	14	8
5 10	19	8	16	3
10 15	12	10	12	3
15 20	5	10	7	9
20 25	1	12	5	14
25 30	3	3	3	11
30 35	2	7	4	6
> 35	8	7	8	37
N	136	60	196	65

Table 16. Percentage occurrence of discrepancies between the POLAN and CCIR values of ymF2 for different ranges of X.

4.0 INDICATORS OF PROFILE QUALITY

4.1 Determination of M(3000)F2

As described previously, the value of M(3000)F2 is obtained by dividing the maximum value of the product f•m by foF2. The derived value of M(3000)F2 will be suspect to some extent if the maximum of f•M occurs at the last scaled frequency below foF2. Examination of the ionograms indicates that this usually occurs when there is very little or no F2 cusp. This occurred when the cusp was very small or weak, but also when software errors truncated the trace well below foF2, or the scaled trace was actually an Es trace.

Any errors in M(3000)F2 and the Dudeney value of hmF2 are obviously going to be related, since the latter is based on the former. For the 42 cases with dM ranging from 0 to 0.1 (night) for which the maximum occurred at the last scaled frequency, the median discrepancy between the POLAN and Dudeney values of hmF2 was +17.5 km (POLAN - Dudeney). The median discrepancy for all cases for the same range of dM values was about -15 km. For the 35 cases with dM lying between 0.11 and 0.5, the median discrepancy was +27.5 km, in contrast with the 0 km obtained for all cases with the same range of dM values.

Cases with uncertain M values thus gave rise to discrepancies 30 km higher than the average, and in fact accounted for just over half of the discrepancies which exceeded +30 km. At night, the effect tended to counteract part of the systematic overestimation of hmF2 by the Dudeney method.

The fact that the scaled value of M(3000)F2 comes from the last scaled frequency below foF2 is thus a good indicator that the F2 cusp and the derived N(h) profile around the F2 peak are unreliable.

4.2 Discrepancies Between POLAN and Dudeney Values of hmF2

The discussion in preceding sections suggests that discrepancies between the POLAN and Dudeney values of hmF2 can be used directly as a quality control indicator for the auto-scaling. Examination of the ionograms and the auto-scaled traces for those cases in which the discrepancy exceeded 30 km showed that the bulk of the ionograms had been incorrectly scaled by ARTIST for various reasons. The figure of 30 km may thus be taken as a good first estimate of the upper limit of acceptable discrepancies. Since this would bring into question some nighttime profiles which are in fact scaled correctly, because the Dudeney value is systematically low at night, some effort should be made to refining this estimate further. This effort should be preceded by improvements of the Dudeney-type models for nighttime conditions, but this will not be attempted here.

4.3 Discrepancies Between POLAN and CCIR Values of ymF2

For $X \leq 6$, the discrepancies between the POLAN and CCIR values of ymF2 for the Richfield data had a median value of +5 km, with 2/3 of the discrepancies lying within 15 km of this value. Values lying more than 25 km from the median value can be considered unreliable.

For $X > 6$, the sample size was too small (65) and the number of cases with discrepancies exceeding 35 km (37) too large to allow a reliable distribution of the errors to be deduced. However, at least those ionograms for which the discrepancies exceed 35 km should be considered unreliable.

4.4 Standard Errors in hmF2

POLAN lists twice the standard error in the calculated values of foF2 and hmF2 in the array positions

FV(N+1) and HT(N+1) [Titheridge, 1985; Section 10.3.1]. We have saved the latter for use as a quality indicator. It is labelled STER in Tables 2 to 6. Note that these errors indicate the accuracy of the least-squares peak fit, and give no indication of systematic data errors or the effects of real height errors at lower frequencies. The standard error in the POLAN value of foF2 (which is not constrained to remain the same as the specified value) could also be used, but the two errors would be very closely related.

For $0 < dM \leq 0.1$ (night), 45% of the 60 cases with values of STER greater than 10 km (60 out of 309 cases) had discrepancies between the POLAN and Dudeney values of hmF2 exceeding the upper or lower bin values. For $0.11 < dM \leq 0.5$ (day), 19% of the 59 cases with values of STER greater than 10 km (59 out of 474) had similar discrepancies. At night, the median discrepancy rose from about -12.5 km to about +12.5 km, while during the day it rose from about +2.5 km to about 17.5 km. Large values of STER are thus associated with extreme values of the discrepancies and with a general increase of 15 to 20 km in the median values of the discrepancies. They can therefore be considered as indicating a class of results different from the average class, and in general indicating an error in the calculated N(h) profile. A much more comprehensive data base would be required to quantify further the relationship between STER and the probability of an incorrect N(h) profile having been calculated.

4.5 Model Values of the Scale Height

The Chapman peak fitted to a layer peak by POLAN is expressed (exactly) as a parabolic peak plus a correction term. The latter is determined by iteration, beginning with

a model value SHA for the scale height. Only one iteration is used, so the results still have some dependence on SHA. The correction term disappears at the peak, and is large at lower frequencies. Thus when good data are available to within about 8% of the critical frequency, the final scale height SH is almost independent of SHA. When the highest scaled frequencies are further below FC (foF2), the calculated SH is increasingly biased towards SHA. Thus as the available data get too far below the peak to give a reliable estimate of peak curvature, the assumed curvature (defined by the scale height) tends to the model value. If the estimate of the peak curvature is too uncertain, POLAN sets the printed value of the scale height negative.

A negative value of the scale height provided by POLAN is thus another indicator that the peak fit is uncertain, and that the deduced N(h) profile is uncertain, at least near the peak. We have not studied in detail the cases for which POLAN defaults to the model value of the scale height.

5.0 SOURCES OF ERRORS IN THE N(h) PROFILES

It is not intended that every unreliable N(h) profile encountered be considered in detail here, since many of those caused by failures of the auto-scaling software have already led to the required changes being implemented in ARTIST. The interested person can work his way through Tables 2 to 7, examining each ionogram for which any of the four (model scale heights were not flagged in the analysis) quality control indicators suggested that the N(h) profile was unreliable.

There will always be some ionograms which will be incorrectly scaled by ARTIST. These will correspond to special ionogram morphologies and ionospheric conditions, and will also be largely un-scalable by a human scaler.

Table 17 shows the breakdown of reasons for the unreliable N(h) profiles in the 59 (out of 977, or 6%) cases for which all three of the following indicators indicated an unreliable result:

1. A discrepancy between the POLAN and Dudeney values for hmF2 lying more than 20 km outside the discrepancy defined by

   dhmF2 = 12.5 - 5 X,

   or less than -30 km.

2. A standard error STER in the POLAN peak fit greater than 10 km.

3. An M(3000)F2 corresponding to the last scaled frequency below foF2.

There were 59 such cases. The fact that there were none for the Goose Bay ionograms may be partly a reflection

	LOW	ARG	UTAH	ERIE	N
Total Ionograms	100	346	276	182	977
Bad Results	17	16	19	7	59
Noise	3	0	0	0	3
Tape - Disk	0	0	4	0	4
Ionosphere	5	0	6	4	15
F2 Cusp	6	2	5	2	15
Discontinuity	2	6	0	0	8
Second Hop	0	0	1	1	2
Poor Scaling	0	6	3	0	9
Miscellaneous	1	2	0	0	3

Table 17. Causes of the poor N(h) profiles for the 59 cases for which three quality control indicators all indicated probable errors in the profiles. There were no such errors for the 72 Goose Bay ionograms.

of the fact that ARTIST has been "trained" on Goose Bay ionograms, but special difficulties were encountered at Lowell (high noise levels; poor transmitting antenna), Richfield (multiple-hop range-spread Es) and Eire (ionospheric storm). Seven general reasons have been found for the poor results - high noise levels (3 cases), technical problems transferring data from tape to disk (4), unusual ionospheric conditions (15), poor scaling of a weak F2 cusp (15), a discontinuity in the scaled trace as the F2 cusp is reached (8), scaling of the second hop echo in place of the first hop (2), incorrect scaling for no good reason (9) and miscellaneous (3). Note that some second-hop scalings were removed in a preliminary examination of the ionograms, as were some long runs of very poor ionograms (Lowell and Richfield, from about midnight to dawn). Thus any detail in the results in Table 17 should not be considered representative. However, the fact that just over half of the problems could be traced to the ARTIST software is probably a reliable statistic.

In the set of ionograms used for the present analysis, ionograms at Richfield were wrongly scaled when the F trace was almost completely obliterated by multiple-hop range-spread sporadic E from around midnight to dawn. One third of the extreme errors obtained for ymF2 corresponded to this situation. For most of the period, ARTIST could not detect a suitable trace at all. Another sixth of the extreme errors were caused by poor scaling of a badly defined F2 cusp. In both of these situations, it is the ionosphere which prevents the derivation of an accurate N(h) profile.

The first day of the Erie ionograms was a geomagnetically disturbed day, during which foF2 was depressed and the F2 trace was weak and at high virtual heights. In many cases, ARTIST scaled the F1 trace as the F2 trace, or at best missed the F1 cusp. The ionograms started to become more

tractable around 1804 UT, although ARTIST encountered problems for another hour or so. There were 24 ionograms analyzed for times before 1804. As can be seen from Table 6, 13 of these results could have been considered questionable because of the large values of DIFF(>30) or STER (>10), or the negative value given for M(3000)F2. A further eight results could also have been questioned if the restriction on DIFF is lowered to 20 km, a value which was exceeded on only 9% of occasions for all the ionograms analyzed.

This left only three results which did not appear questionable - for the 1729, 1734 and 1744 UT ionograms. However, examination of the ionograms and the auto-scaled traces showed that the trace was wrongly scaled at 1729 and 1734, while the F1-F2 trace on the 1744 ionogram defied human interpretation. This suggests that a sequence of ionograms for which the quality control indicators indicate unreliable N(h) profiles can be used to question intermediate N(h) profiles which (probably fortuitously) appear to be reliable, and also to indicate periods of ionospherically disturbed conditions.

6.0 CONCLUSION

This study has shown that the five parameters listed in Section 1.0 can be used as quality control indicators for N(h) analyses of automatically scaled ionograms. About 10% of the ionograms analyzed would have been rejected on the basis of these indicators. In about half of these cases, the problems encountered could be attributed directly to errors in the autoscaling software, which have since been corrected. These errors had previously gone undetected.

It is recommended that the results of this study be refined further, now that some of the sources of error have been eliminated, using a larger and more diverse data base. The present study should be regarded as preliminary and qualitative, to be followed by a quantitative study which will provide explicit procedures for rejecting N(h) profiles on the basis of the values of the five parameters. A parallel study should also be made of methods to eliminate the systematic errors in the Dudeney values of hmF2 at night by allowing for the underlying ionization.

Values of hmF2 given by the simple Dudeney formula could, as an interim measure, be increased by the value:

$$dhmF2 = 12.5 - 5X$$

where $X = foF2/foE$, and dhmF2 is constrained to exceed -20 km.

7.0 ACKNOWLEDGEMENTS

I would like to acknowledge the assistance of Ms. Jane Tang in willingly providing me with the large volumes of autoscaled traces and printed ionograms, and Drs. B. W. Reinisch and G. S. Sales for many helpful discussions during the analysis.

8.0 REFERENCES

Bradley, P. A. and J. R. Dudeney, "A simple model of the vertical distribution of electron concentration in the ionosphere," J. Atmos. Terr. Phys., 35, pp. 2131-2146 [1973].

Dudeney, J. R., "The accuracy of simple methods for determining the height of the maximum electron concentration of the F2 layer from scaled ionospheric characteristics," J. Atmos. Terr. Phys., 45, pp. 629-640 [1983].

CCIR, "Second CCIR computer-based interim method for estimating sky-wave field strength and transmission loss at frequencies between 2 and 30 MHz," Supplement to Report 252, International Radio Consultative Committee, International Telecommunication Union, Geneva, Switzerland [1980].

McNamara, L. F., "A comparative study of methods of electron density profile analysis," World Data Center A for Solar-Terrestrial Physics Report UAG-68, Boulder, CO [1978].

Paul, A. K., "Processing of digital ionograms," Naval Ocean Systems Center Report, *NOSC-TD-529, San Diego, CA* [1982].

Piggott, R. W. and K. Rawer, "U.R.S.I. handbook of ionogram interpretation and reduction," World Data Center A for Solar-Terrestrial Physics Reports UAG-23 and UAG-23A, Boulder, CO [1972].

Reinisch, B. W. and Huang Xueqin, "Automatic calculation of electron density profiles from digital ionograms. 3. Processing of bottomside ionograms," Radio Science, 18(3), pp. 477-492 [1983].

Reinisch, B. W., R. R. Gamache and J. S. Tang, "Automatic electron density profiles from digital ionograms," AGARD, Conference Proceedings No. 345, "Propagation factors affecting remote sensing by radio waves" [1984].

Shimazaki, T., "World-wide daily variations in the height of the maximum electron density in the ionospheric F2 layer," J. Radio Res. Labs., Japan, 2(7), pp. 86-97.

Titheridge, J. E., "Ionogram analysis with the generalised program POLAN," World Data Center A for Solar-Terrestrial Physics Report UAG-93, Boulder, CO [1985].


DATE
FILMED
0-8